Statistical Analysis of Hartmann-Shack Images of a Pre-school Population

by

Damber Thapa

A thesis
presented to the University of Waterloo
in fulfillment of the
thesis requirement for the degree of
Master of Science

in
Vision Science

Waterloo, Ontario, Canada, 2010

Author's Declaration

I hereby declare that I am the sole author of this thesis. This is a true copy of the thesis, including any required final revisions, as accepted by my examiners.

I understand that my thesis may be made electronically available to the public.

Abstract

The impact of uncoordinated growth of the optical components of the eye may stimulate different levels of monochromatic aberrations in the growing eyes of the children. This thesis aimed to examine the impact of age, visual acuity and refractive error on higher order aberrations as well as to determine the relationship between them.

Hartman Shack images taken with the Welch Allyn® SureSight Autorefractor were calibrated in order to determine the Zernike coefficients up to the 8th order for a pupil diameter of 5mm. The MATLAB code proposed by Thibos et al that follows the standard for reporting the optical aberrations of the eye was the basis of code written for this study. Modification was required to suit the specific needs of the Welch Allyn® SureSight Autorefractor. After calibration the lower order aberrations could then be compared with the results from cyclopledged retinoscopy. RMS values of aberrations and Strehl ratios were computed to examine the optical performance of the eye.

A total of 834 Hartmann-Shack images of 436 children (mean age 3.94± 0.94 years, range 3 to 6 years) were examined in this study (right eyes 436; left eyes 398).The sample had a mean (± STD) spherical equivalent of 1.19 ± 0.59D, a mean with-the-rule astigmatism (J_0) of 0.055 ± 0.22D, and a mean oblique astigmatism (J_{45}) of 0.01±0.14D. Visual acuity varied from 6/6 to 6/18.

Moderate mirror symmetry was found between the eyes. Like refractive error, higher order aberrations declined with age in this sample. There was an impact of higher order aberrations on refractive error. Significantly higher ocular aberrations were found in the higher hyperopic group (SE>+2.0D) compared to emmetropic (-0.5<SE<+0.5D) and low hyperopic groups (+0.5<SE<+2.0D). The Strehl ratio was significantly lower in the high hyperopic group. Higher Strehl ratios were observed for better acuity groups but the average Strehl ratios among the different visual acuity groups were not statistically significant.

In conclusion, there was an impact of age on the ocular aberrations. A wider range of age from birth to adolescence is required for further investigation. This could be indirectly influenced by the age related changes in refractive error as the correlation between refractive error and the higher order aberrations were significant. This finding also concludes that Strehl Ratio alone is not capable of perfectly describing the visual acuity of the eye; other metrics such as the neural transfer function and neural noise are necessary to describe the resultant visual performance of the eye.

Acknowledgements

In the first place I would like to recode my sincerest gratitude to Dr. Vasudevan Lakshminarayanan and Dr. William R. Bobier for their encouragement, guidance and support from the initial to the final level which enabled me to develop an understanding of the subject. It is an honor and great pleasure for me to work under their supervision.

Thank you to my committee members, Dr. Trefford Simpson and Dr. Marlee Spafford, for their assistance and constructive comments on this thesis.

I am very grateful to Mr. Andre Fleck for calibrating the instrument and his willingness to share his bright thoughts with me. I am grateful in every possible way and hope to keep up our collaboration in the future.

This study was supported in part by an industrial grant to W.R. Bobier from the Welch Allyn Company. Thank you.

It is a pleasure to express my appreciation heartily to Dr. Lakshminarayananan's family especially to Annette McBride for her encouragement and support in various ways. I convey my special thanks to Krista Parsons for her precious help dealing with administration. Thanks to Mirka Curran and the entire library staff for their assistance.

Many thanks go to my lab mate Azadeh Faylienejad for giving me such a pleasant time when working together with her. Special thanks to my housemates Sumit and Gaurav for creating a homely atmosphere.

I am indebted to my family. This thesis would not have been possible without their love and support. Finally, I would like to thank everybody who supported me in any respect during the completion of this thesis.

Table of Contents

List of Figures

List of Tables

Chapter 1
Introduction

1.1 The Human Eye

The human visual process starts with the formation of the retinal image by the optical components of the eye. The light coming from an object is refracted by the optics of the eye, mainly by the cornea and crystalline lens and focuses on the retina. Light is refracted first by the cornea which is a positive lens of fixed power that varies with age. The first surface of the cornea is the tear film that works as a lubricant and is essential for maintaining corneal integrity and transparency[1,2]. Since the difference in index between the cornea's interface with air is greater than that of the lens surrounded by aqueous and vitreous, the power of the cornea is greater than that of lens and hence light is refracted more by the cornea. The shape of the cornea is not perfectly spherical rather it is aspheric. The peripheral region is flatter than the central region; however, for simplicity the radius of the cornea is approximated as 7.8 mm for the anterior surface and 6.4mm for the posterior surface which makes the total power of the cornea nearly equal to 42.2D[1]. Furthermore, horizontal and vertical curvatures of the cornea are not equal; this toricity in the human cornea produces astigmatism[1].

The aqueous humor does not contribute to the refraction of light as its refractive index is very close to the index of the cornea; however, its correlated growth with the power of the eye controls the refractive error of the eye[1]. The iris of the eye works as an aperture and the central opening is called the pupil. The pupil controls the amount of light entering to the eye by changing its diameter. Its diameter varies from about 2mm in very bright light to 8mm in the dark[1]. The light is further refracted by a transparent, high refractive index material called

the crystalline lens. The lens is composed primarily of proteins and disruption of these protein structures leads to cataract formation[3]. Shape of the lens is responsible for changing the curvature and hence focusing the object of regard on the retina. It should be noted that the lens has a gradient index profile. It is less at the edge and increases continuously towards centre[3]. With age, the lens index increases and becomes more rigid and hence there is a loss in flexibility. This condition is called presbyopia. The power of the lens varies in order to focus on objects at different distances. The process of changing the power of the eye in order to focus the object of regard on the retina is called accommodation[1]. Generally the range of accommodation varies from infinity to the near point of the eye. After the lens, the refracted ray passes through the vitreous humor and imaged on the retina. The retina consists of optically sensitive photoreceptors which transduce the light into electrical impulses and the impulses are carried by the optical nerve to the brain to complete the visual process.

1.2 Refractive Error

The human eye is not a perfect optical system[4]. Rays of light coming from a distant object may not always focus on the retina. An unaccommodated eye which focuses parallel rays of light on the retina is termed as emmetropic eye[5] (Fig 1.1 a). The eye which is not emmetropic has a focusing error[5]. This focusing error is called refractive error. The effect is purely optical and can be corrected by simple means such as a spectacle lens, contact lens or refractive surgeries. Basically, refractive error is categorized into two types, spherical refractive error and astigmatism[5]. In the spherical refractive error, the optics of the eye is capable of forming the sharp image; however, the image is not on the retina, but is either in front of or behind the retina. These eyes are different from the emmetropic eyes either in

terms of refractive power, axial length or both[5]. With age, refractive index of the lens also plays an important role to induce refractive error. The mismatch between the axial length and refractive power of the eye creates a blurred image on the retina and vision is adversely affected[5].

If the power of the eye is too high or the axial length of the eye is too long, parallel rays of light focus in front of the retina and this error of refraction is called myopia (Fig 1.1b). Myopes can not see objects beyond certain limiting point called the far point. However, they can see an object at closer distances until the focus ends. The closest object point they can see is called near point[5]. Myopia is often refered to as short-sightedness[5]. The object in front of a myopic eye can be brought into focus on the retina by using a negative lens of appropriate power. If the power of the eye is too low or the axial length of the eye is too short, light from the object focuses beyond the retina and this error of refraction is called hypermetropia or simply hyperopia (Fig 1.1c). Hyperopes do not have any problems for distant objects but can not clearly see an object at closer distances and hence hyperopia is often referred to as far-sightedness[5]. The object in front of a hyperopic eye can be brought into focus on the retina by using a positive lens of appropriate power.

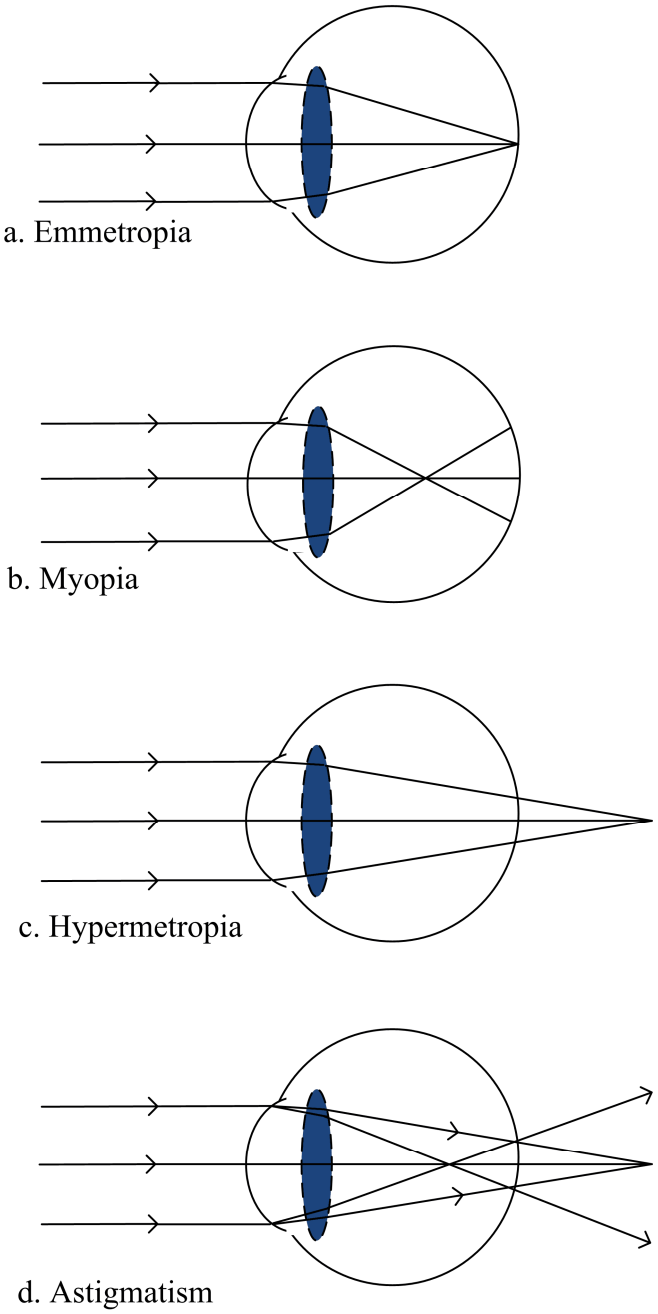

Figure 1:1 Schematic eye with (a) Emmetropia (b) Myopia (c) Hypermetropia and (d) Astigmatism

The optical components of the eye develop from birth to adolescence[6]. The axial length of the neonate's eye is around 17mm which continuously grows and matches with the secondary focal length of the eye at the time of emmetropization[7]. The exact axial length of the eye varies between studies, techniques and individuals[6]. The growth is rapid in the first two years of life where the increment is around 3.8mm and gradually increases from 2 to 5 years where the increment is around 1.2mm[6]. The axial growth of the eye is mainly due to the vitreous chamber growth; with about 62.5% of the total axial length of the neonate's eye is due to the vitreous chamber length which increases and by the age of 13 years, 69.5% of the total axial length is due to the vitreous chamber length[6]. The anterior chamber length also increases but the increment is not as big as the vitreous chamber. The anterior chamber length increases by 1.4 mm from birth to the teen years[6]. The retinal image size of the infant's eye is about 3/4 the size of the adult eye as the average size of the visually normal infant's is about 3/4 the size of the adult eye[7]. It should be noted that as the image size decreases the detail of the image decreases. With increase in age of the children, the retinal image size as well as detail of the image increases[7]. The average corneal power of neonate's eye is 48D, which gradually decreases with growth and becomes around 44D by the time the child is 2 years of age[7,8]. The power of the crystalline lens also drops down from birth to adolescence. The average 45D power during birth time drops off by 20D by the time the child is 6 years of age[7,9].

The coordinated growth of the optical components of the eye controls the refractive error so that a state is reached where the focal length of the eye exactly matches the axial length of the eye. This is known as emmetropization. In general for an adult eye, 1mm change in axial

length correlates with about 2.7D changes in refractive power[5]. Previous studies[10-12] show that corneal curvature correlates with the axial length of the emmetropic and myopic eye. If the axial length is greater, then the cornea tends to be flatter[13]. Myopes have steeper central corneal curvatures, deeper anterior and vitreous chambers, and greater axial lengths compared with emmetropes[11].

Banks[14] in 1980 reviewed 11 other studies and showed that the average newborn infant is hyperopic with a mean (± standard deviation) refractive error of around 2.0±2.0 D. Banks also showed that the variation of refractive error is least at the time of emmetropization. Other studies also found a small amount of hyperopia with a smaller amount of standard deviation by the age of 6-8 years[13]. For example, Hirsch[15] observed mean hyperopia of 1.0±1.6D at the age of 8 years. Only a small number of children are born myopic at birth. As the age increases the degree of both the myopia and hyperopia decreases in the first few years of life and the child becomes close to emmetropic at the age of 6 years[16]. Unlike hyperopia, average myopia shifts to low hyperopia in the preschool years and after that it also decreases and slowly experiences emmetropia[16, 17]. In general, refractive error changes from hyperopia through emmetropia to myopia in school years[13] and hence most of the adults are emmetropic or slightly myopic[18]. The variation of refractive error in adults has been described in several cross-sectional population-based studies; however, it is difficult to find large scale longitudinal studies which deal with the variation of refractive error from 20-40 years of age. Data reported to Grosvensor[18] by optometrists who followed their own refractive errors in 5 years increments have shown that most of the adults are emmetropic or slightly myopic in nature and there is not much change in refractive error from 20-40 years of age. Studies of

refractive error in individuals over 40 years have shown increasing prevalence of hyperopia with age[19, 20, 21]. For example, the Beaver Dam eye study[22] found a clear shift towards hyperopia of +0.28D from 43 to 84 years. The prevalence of hyperopia is greater than that of myopia, which ranges from 36% to 57%[23,24]. In general, the prevalence of myopia in visually normal adults is about 12.6% to 18% but it varies with race[25]. The prevalence of myopia is high in the East Asian population with a rate of 28% followed by the European population with a rate of 26.5%[25]. It should be noted that the refractive measures depend upon whether the refraction is performed with or without cycloplegia; the measurement in children and infants is also influenced by autorefractor design[26].

When the refracting surface is astigmatic there are two perpendicular power meridians (figure 1.1 d). The power of the surface varies from a minimum in one of the meridians to a maximum in the others[1]. Astigmatism is the difference in power between the two mutually perpendicular power meridians. The astigmatic surfaces do not form a point image of an axial object. In the human eye, astigmatism is mostly caused by the anterior corneal surface[1]. This appears to be the same during early development as well[27]. If the power of the vertical power meridian is greater than that of the horizontal power meridian, then this type of astigmatism is called with-the-rule astigmatism; whereas if the power of the horizontal power meridian is greater than that of the vertical power meridian, it is called against-the-rule astigmatism. The pattern of astigmatism varies somewhat in differing populations but astigmatism emmetropizes during the first 2 to 3 year of life[27-29]. By preschool age, with-the-rule astigmatism becomes the more frequent pattern[6, 30]. Gwiazda et al.[31] studied the infant eye and observed that 56% of the children have significant amounts of astigmatism, which

reduces to less than 5% at preschool age. Dobson et al.[32] observed high prevalence of astigmatism in infants and toddlers, and that vanishes by the time the children reach school age.

1.3 Visual Acuity

In the human eye, the object is normally located beyond twice of focal length (2f), so according to the geometric optics, the image size is always smaller than object. When an object such as an alphabet letter is large, the detail of its retinal image is easily recorded. When the size of the object decreases, the retinal image as well as the detail of the retinal image also decreases until the retinal image becomes so small that the visual system can not recognize the letter. Visual acuity is the finest detail that can be perceived by the observer[13]. The average visual acuity of the neonate eyes is approximately 1 cycle per degree, which quickly improves and by the age of 1 month, children usually attain around 5 cycles per degree and by the age of 8 month it becomes 16.3 cycles per degree vision[13]. This VA gradually improves and by the age of 5 years children usually have 30 cycles per degree vision[7,33,34]. The development of visual acuity results from improvements in the optics of the eye, the shape, size and distribution of the retinal photoreceptors[35], the myelination of visual pathway and the increase in the number of synapses[36]. For pre school children, letter matching tests are frequently used to assess visual acuity, where the child's task is to match the letters on the screen to those on a matching board. Several versions of letter matching charts exist with single and/or crowded letter presentations[13]. One of the most useful letter matching tests is the Cambridge Crowding Cards test; it is descried more detail in Chapter 2.

Visual acuity is affected both by optical and neural factors. During infancy, the visual pathway is still developing so the visual acuity is very poor. The retinal area responsible for fine detail resolution is the fovea, which develops as the child grows. The fovea is composed in part of photoreceptors called cones. The greater the density of cones, the sharper the vision is because resolution increases with cone spacing and layout[7]. The most sensitive part of the fovea is called the foveola. The size of the foveola decreases with age but there is a greater concentration of cones in this area. The density of cones in the child's fovea is less than one fourth of that in the adult fovea[7]. Furthermore, there are significant maturational changes in the visual pathways and in the cerebral cortex over the first 3 to 6 months of life that underlie significant improvements in visual acuity[36]. When photoreceptors transduce photons into electric impulses, they are transmitted to the brain by the optic nerves. The myelin, which covers the nerve fibres, improves the transmission of neural signals to the adjacent nerves. In the infants, the nerves are not fully myelinated[7].

Visual acuity is affected by ocular aberrations and diffraction. For large pupil sizes, aberrations increase and degrade the retinal image quality; whereas in small pupil sizes, a point object is imaged as a circular patch called the Airy disk[5]. The size of the Airy disk increases in the diffraction-limited system resulting in decreased central vision and degraded retinal image quality. Visual acuity is poor for very small pupils (less than 2mm) as well as for very large pupils. For the best visual acuity, the optimal pupil size is about 3mm[5].

1.4 Wavefront Aberration

The visual process is associated with both optical and neural factors. The quality of the retinal image is affected by many factors such as diffraction, scattering, refraction, accommodation, as well as monochromatic and chromatic aberrations[4]. Very little has been done to improve the quality of vision caused by diffraction, scattering and chromatic aberration[4]. Chromatic aberration is due to the variation in refractive index of the eye with the wavelength of light. Monochromatic aberration can be measured, described and analyzed from wavefront measurements[4].

The wavefront is defined as the locus of points in the wave which are all in the same phase[38]. The wavefront can also be defined as the surface of constant optical path lengths (i.e. product of physical length and refractive index of the medium). So it does not require that wavefronts always have to be spherical; however, they must be surfaces of constant phase. The phase of wavefronts may change when they pass through different optical media but they change uniformly over the entire surface. The plane or spherical wavefront is taken as the ideal or reference wavefront from which to compare other wavefronts[38].

An optical system such as a lens is capable of changing the shape of the wavefront[37]. For example, a convex lens transforms incoming wavefront into a converging wavefront and a concave lens transforms incoming wavefront into a diverging wavefront. A perfect optical system can transform an incoming wavefront into a perfect spherical convergent wavefront[38]. Only a spherical wavefront can be focused as a diffraction-limited Airy-disk (Fig 1:2 left side). The imperfect or aberrated optical system can not transform an incoming wavefront into a complete spherical wavefront. Fig 1:2 (right side) shows that each point in the

converging wavefront is in the same phase; however, the wavefront is not spherical. Such a non-spherical wavefront is called an aberrated wavefront[38].

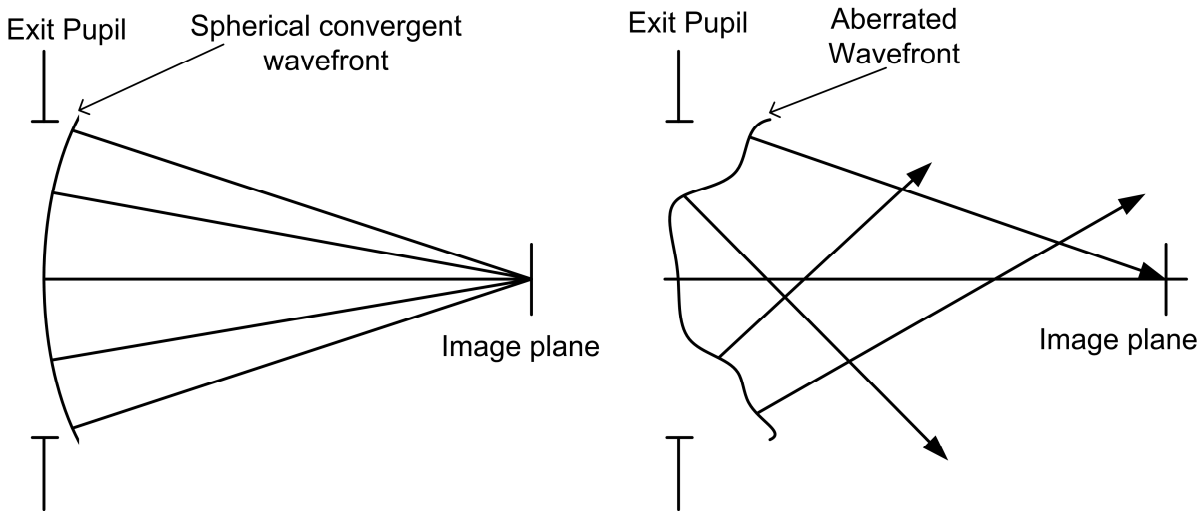

Figure 1:2 A spherical convergent wavefront converges at a single point (left side). An aberrated wavefront does not converge at a single point so a point image is not formed (right side).

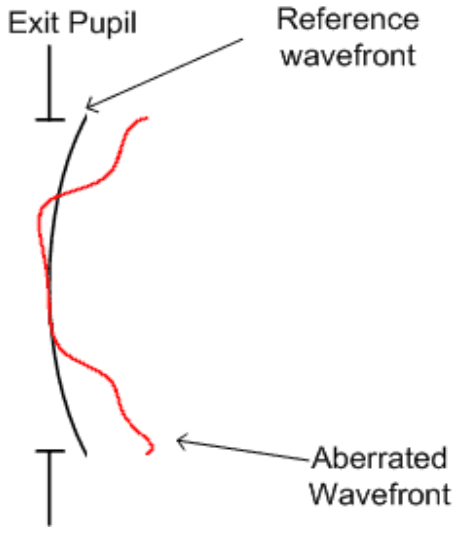

Figure 1:3 Wavefront aberration is the optical path difference between the ideal and the aberrated wavefront.

Wavefront aberration is defined as the optical path difference between the ideal wavefront and the aberrated wavefront. These two wavefronts coincide at the centre of the exit pupil where the wavefront aberration is zero but depart at other parts of the exit pupil (Fig 1:3). If the aberrated wavefront leads the reference wavefront then it is considered positive; whereas if it lags the reference wavefront then it is negative[4]. This can be observed by the different color codes of a contour plot. Different colors represent the departure of an aberrated wavefront from the reference wavefront (Fig 1:4). The optical path difference of each point over the entire exit pupil gives a function W(x,y) which is called a wavefront aberration and can be used to describe the aberrated wavefront[38]. Wavefront aberration is measured either in microns or as a fraction of wavelength and is expressed as the RMS (root mean square) value. This wavefront aberration can be used to derive a point spread function, which is the image of a point object formed by the optical system. The modulation transfer function (MTF) can be derived from a point spread function to examine the effect of aberration on the image quality of the eye.[39]

The ocular aberration was first measured by Smirnov,[40] who demonstrated the measurement of the ocular aberrations by using Scheiner double pinholes. This subjective method was able to show the different levels of ocular aberration present in the human eye. Later, Howard and Bradford[41] developed a subjective method to measure the ocular aberration that was the most reliable method at that time. They used Zernike coefficients to describe the aberrations of the eye and observed that third order coma-like aberrations were significant in the higher order aberrations. Their cross-cylinder aberroscope was a subjective

method which depended upon the performance of the subjects so it was modified later by Walsh et al[42] in order to measure the ocular aberration objectively. Later Mierdel and Mrochen[43] used the principle developed by Tscherning at the beginning of the 20th century to create an objective method that calculated the aberration of the eye in clinical conditions.

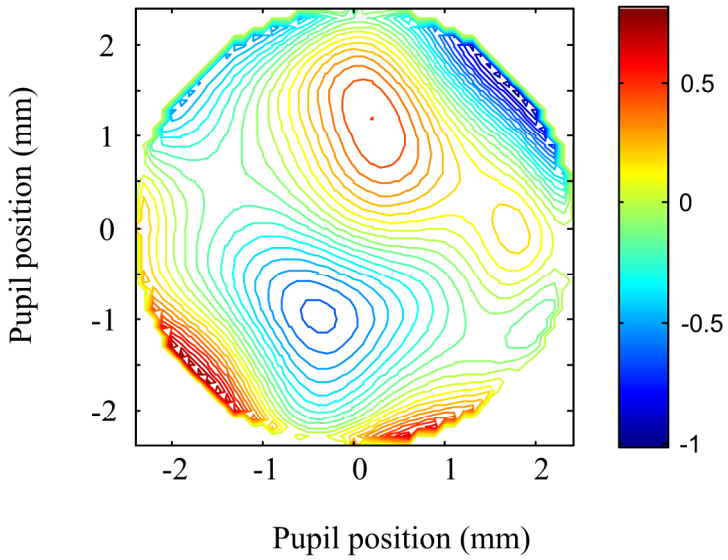

Figure 1:4 Contour plot showing the departure of the aberrated wavefront from the reference wavefront

Most recently, the Hartmann-Shack[44] method has been introduced and has become extremely popular. Hartmann, a physicist at the end of the 19th century, introduced a method based on ray tracing that reconstructs the entire wavefront by integrating the local slope of the wavefront. Ronald Shack at the University of Arizona used this method with a Charged Couple Device (CCD); this approach was initially used in astronomical telescopes to remove the distortion caused by atmospheric turbulence. The Hartmann-Shack wavefront sensor was used by Liang et al.[44] to measure the aberration of the eye. In this method, light reflected from the retina is captured outside the eye (Fig 1:5).

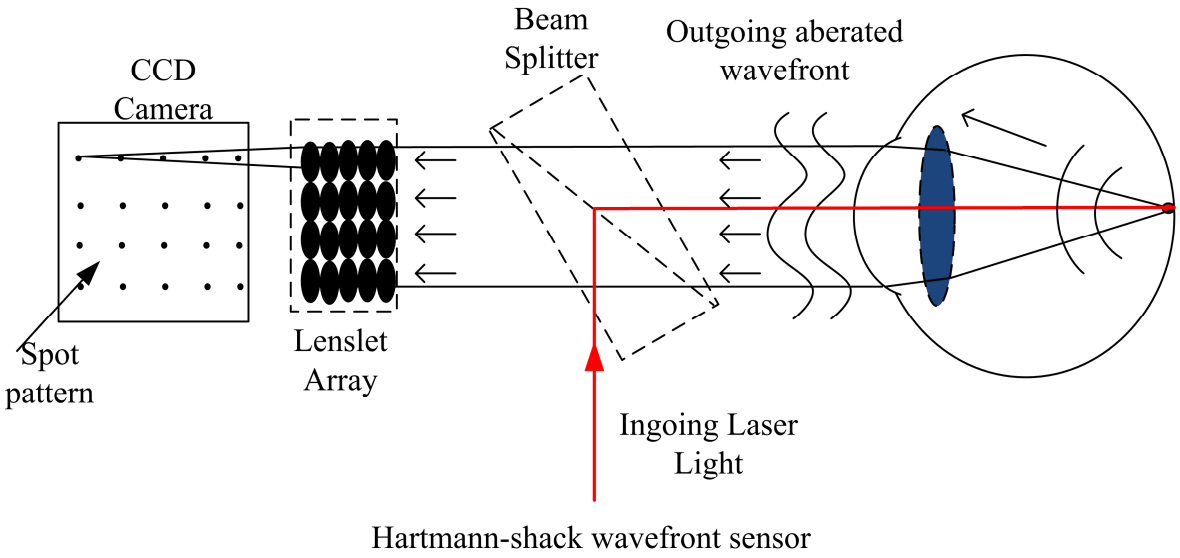

Figure 1:5 Schematic diagram of Hartmann-shack wavefront sensor.

Three different types of aberrometers are commercially found in the market. The first kind of are those based on subjective methods in which measurements are taken for ingoing light such as spatially resolved refractometer.[45] The second type of aberrometer is based on objective methods in which measurements are taken for ingoing light. Examples include the cross cylinder abberroscope[41] and the Tscherning abberroscope[43]. The third type of aberrometers are based on objective methods in which measurements are taken for outgoing light such as Hartmann-Shack wavefront sensor[44]. The more detailed pictures of different types of aberrometers can be found in the third chapter of the book *Adaptive optics for vision science*[46].

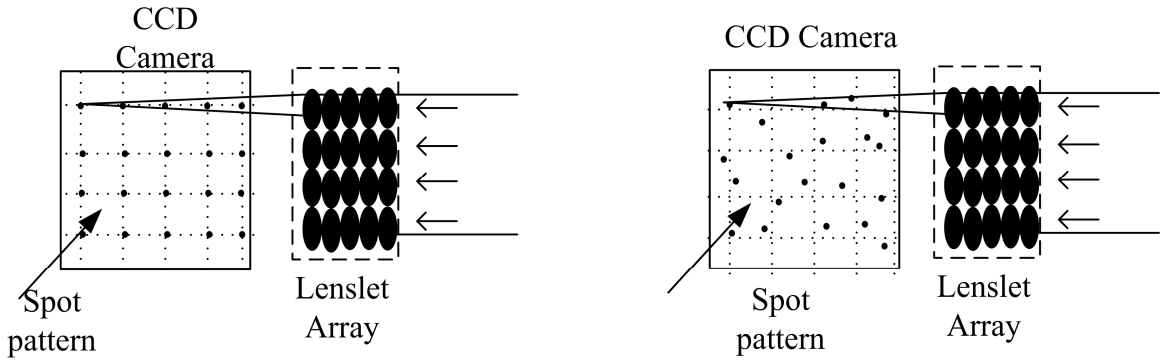

Figure 1:6 Spot patterns of ideal (left side) and aberrated eye (right side)

In the Hartmann-Shack method, laser light is sent into the eye to produce a small quasi-point source of light on the retina. The light reflected from the retina passes through the lens and cornea and leaves the eye. If the eye were a perfect optical system (i.e. free from aberration) the rays of light emerging out of the eye would be parallel and the wavefront would become flat. The emerging wavefront hits the Hartmann-Shack wavefront sensor which consists of identical lenslet arrays of equal focal length. The wavefront is then divided into the number of sub-apertures and imaged onto the CCD camera placed at the focal plane of the lenslet array. Each lenslet images a spot onto the CCD camera. If the wavefront emerging out the eye is plane then each lenslet produces its spot exactly at its optical axis and the spot patterns are exactly the same as reference grid (Fig 1:6 left side). The spot patterns of the aberrated wavefront (Fig 1:6 right side) are displaced from their optical axis and the displacement of each spot is proportional to the local slope of the wavefront. The slope of the aberrated wavefront W(x, y) at an arbitrary point (x, y) is given by the following relationships[39,44].

$$\frac{\partial W(x,y)}{\partial x} = \frac{\Delta x}{f}$$

$$\frac{\partial W(x,y)}{\partial y} = \frac{\Delta y}{f}$$

Where Δx and Δy represent the shifts of the spot from its optical axis at points (x, y) and f is the focal length of the lenslet.

This indirect measurement of the local wavefront slope from the measurement of the displacement of the spot is used to reconstruct the entire wavefront by integrating these slopes[46]. The reconstructed wavefront is analyzed to calculate the ocular aberration.

1.5 Aberration description

The wavefront aberration W(x, y) can be described by expanding it in a mathematical polynomial in which each term of the polynomials describes a particular aberration[38]. Taylor polynomials were used to describe ocular aberrations in the past but Zernike polynomials are more widely used now because of their orthogonal property. This study also describes the ocular aberration in terms of Zernike polynomials.

Taylor polynomials describe the wave aberration in terms of object height and pupil coordinates. The Taylor polynomial can be described mathematically as[38,39,47]

$$W = \sum_{k,l,m} W_{klm} h^k r^l \cos^m \theta$$

Where, $k = 2j + m \; and \; l = 2n + m$; W_{klm} represents the wave aberration coefficient of the various terms usually measured in microns or as a fraction of wavelength of the light, h is the height of the object and r and θ are the polar coordinate variables in the pupil plane. The polynomials can be expanded as follows[39]

$$W = [piston] + [tilt] + [W_{020} r^2] + [W_{040} r^4] + [W_{131} h r^3 \cos(\theta)] + [W_{222} h^2 r^2 \cos^2(\theta)] + [W_{220} h^2 r^2] +$$

$$[W_{311} h^3 r \cos(\theta)] + \ldots\ldots\ldots\ldots\ldots\ldots higher\ order\ terms$$

The first two terms (i.e. piston and tilt) are constant terms and do not contribute to the aberrations of the eye. The following six aberration terms are named as defocus, spherical aberration, coma, astigmatism, curvature of field and distortion, respectively and are called Seidel aberrations. This is a traditional way of representing the ocular aberration in which each term of the polynomial represents a particular type of Seidel aberration. However, these polynomials are not independent of each other; variation in one term influences the other remaining terms so these are not recommended. In 1934, the Dutch physicist, Frits Zernike, discovered a polynomial series which meets that demand i.e. they are an orthogonal set of basis function over the interior of the unit circle and each term of the polynomials represents a particular type of ocular aberration and the polynomials are mathematically independent to each other. These have been widely used in astronomy. Zernike polynomials are usually expressed in a polar coordinate system and can be describe mathematically as follows[38,39].

$$Z_n^m(\rho,\theta) = N_n^m R_n^{|m|}(\rho)\cos(m\theta) \qquad for \quad m \geq 0$$

$$= -N_n^m R_n^{|m|}(\rho)\sin(m\theta) \qquad for \quad m < 0$$

Each Zernike polynomial term, $Z_n^m(\rho,\theta)$, consists of three components; a normalization term (N_n^m), radial polynomial ($R_n^{|m|}(\rho)$) and Azimuthal sinusoidal component. The order of the polynomial is represented by n, and m represents the angular frequency of the sinusoidal component. For a particular value of n, the angular frequency m varies from +n, to –n with step sizes of 2 such as n, n-2, n-4,…….-n. The radius vector ρ gives the radius of the exit pupil whose value ranges between 0 and 1. The other angular pupil coordinate, θ, ranges between 0 and 2π. The normalization factor N_n^m is given by[39]

$$N_n^m = \sqrt{\frac{2(n+1)}{1+\delta_{m0}}} \quad where, \delta_{m0} = 1 \; for \; m = 0 \; and \; \delta_{m0} = 0 \; for \; m \neq 0$$

The radial polynomial $R_n^{|m|}(\rho)$ depends upon the radius of the exit pupil and can be expressed as[39]

$$R_n^{|m|}(\rho) = \sum_{r=0}^{(n-|m|)/2} \frac{(-1)^r (n-r)!}{r![0.5(n+|m|)-r]![0.5(n-|m|)-r]!} \rho^{n-2r}$$

Another useful fact about the Zernike polynomials is their orthonormality property. The mean value of aberration over the entire pupil is zero so the coefficient of a particular term is the root mean square (RMS) value of that term. So they are recommended for expressing the ocular aberration[4, 47].

Table 1:1 Zernike polynomials up to forth order

Mode (j)	Zernike Term	Zernike polynomials Polar coordinate	Zernike polynomials Cartesian coordinate	Meaning
0	Z_0^0	1	1	Piston
1	Z_1^{-1}	$2\rho\sin(\theta)$	x	Tilt in x-direction
2	Z_1^1	$2\rho\cos(\theta)$	y	Tilt in y-direction
3	Z_2^{-2}	$\sqrt{6}\rho^2\sin(2\theta)$	2xy	Oblique Astigmatism
4	Z_2^0	$\sqrt{3}(2\rho^2-1)$	$-1+2x^2+2y^2$	Defocus
5	Z_2^2	$\sqrt{6}\rho^2\cos(2\theta)$	y^2-x^2	Radial astigmatism
6	Z_3^{-3}	$\sqrt{8}\rho^3\sin(3\theta)$	$3xy^2-x^3$	Vertical trefoil
7	Z_3^{-1}	$\sqrt{8}(3\rho^3-2\rho)\sin(\theta)$	$-2x+3xy^2+3x^3$	Vertical coma
8	Z_3^1	$\sqrt{8}(3\rho^3-2\rho)\cos(\theta)$	$-2y+3y^3+3x^2y$	Horizontal coma
9	Z_3^3	$\sqrt{8}\rho^3\cos(3\theta)$	y^3-3x^2y	Horizontal trefoil
10	Z_4^{-4}	$\sqrt{10}\rho^4\sin(4\theta)$	$4y^3x-4x^3y$	Vertical quadrafoil
11	Z_4^{-2}	$\sqrt{10}(4\rho^4-3\rho^2)\sin(2\theta)$	$-6xy+8y^3x+8x^3y$	Secondary astigmatism
12	Z_4^0	$\sqrt{5}(6\rho^4-6\rho^2+1)$	$1-6y^2-6x^2+6y^4+12x^2y^2+6x^4$	Spherical aberration
13	Z_4^2	$\sqrt{10}(4\rho^4-3\rho^2)\cos(2\theta)$	$-3y^2+3x^2+4y^4-4x^2y^2-4x^4$	Secondary astigmatism
14	Z_4^4	$\sqrt{10}\rho^4\cos(4\theta)$	$y^4-6x^2y^2+x^4$	Horizontal Quadrafoil

Table 1:1 shows the representation of the Zernike polynomials. The first column is the representation of Zernike modes in terms of a single-indexing scheme, denoted by the value of "j". Column 2 shows the double-indexing system, in which the polynomials are represented by Z_n^m. The polynomials are identified by their superscript "m" and subscript "n"

and represent a particular type of aberration. For example for n=2 and m=0, it represents defocus, in clinical term it is also called spherical ametropia or simply myopia or hyperopia. When n=2 and m=-2 it is called astigmatism with axis either at 90^0 or 180^0, for n=4 and m=0 it represents the spherical aberration. The eye has different types of aberrations; some of them have their own special name like spherical aberration, coma, trefoil etc but most of them are just recognized by Zernike polynomials.

In terms of the Zernike polynomials the wavefront aberration $W(\rho,\theta)$ can be expressed as a weighted sum of the Zernike polynomials[38,39,47]

$$W(\rho,\theta) = \sum_{n}^{r} \sum_{m=-n}^{n} C_n^m Z_n^m(\rho,\theta)$$

$$W(\rho,\theta) = C_0^0 Z_0^0 + C_1^{-1} Z_1^{-1} + C_1^1 Z_1^1 + C_2^{-2} Z_2^{-2} + C_2^0 Z_2^0 + C_2^2 Z_2^2 + C_3^{-3} Z_3^{-3} + C_3^{-1} Z_3^{-1} + C_3^{-1} Z_3^{-1} + C_3^3 Z_3^3 + C_4^{-4} Z_4^{-4} + C_4^{-2} Z_4^{-2} + C_4^0 Z_4^0 + C_4^2 Z_4^2 + C_4^4 Z_4^4 + \ldots\ldots\ldots\ldots\ldots + \textit{other higher order terms}$$

Where, C_n^m is the weighting factor usually called the Zernike Coefficient and represents the amount of aberration present in the particular Zernike mode. The First Zernike term (Z_0^0) is called the piston term and corresponds to the plane wavefront that is longitudinally displaced from the centre[4]. This term is usually ignored because it does not contribute to the aberrations of the eye. The first order aberrations terms Z_1^{-1} and Z_1^1 correspond to the prismatic tilts in which the wavefront is planar but it is tilted about the X-axis and Y-axis, respectively[4]. The prismatic tilts can be minimized by changing the fixation angle and they do not contribute to the quality of images so they are not considered as an aberration of the eye[4]. The aberrations start from second order and have a very large impact on image quality. Some major aberration terms are discussed below.

1.5.1 Defocus

When the secondary focal length of the eye is not equal to its axial length, the wavefront is still a convergent spherical wavefront but the image does not coincide with the position of the retina; it is formed either in front of or beyond the retina, creating a blurred image. In general, defocus refers to the out of focus image[5]. If the eye suffers from defocus, a point object is imaged as a blurred circle which reduces the sharpness and contrast of the image. In more general form, defocus represents myopia or hyperopia. In Zernike polynomials, the defocus corresponds to the coefficient C_2^0 of polynomial Z_2^0.

1.5.2 Astigmatism

As was already discussed, the eye is composed of two perpendicular power meridians; these are the tangential and sagittal power meridians. If the eye has astigmatism, sagittal and transverse rays focus at different distances along the optical axis so the object is not sharply imaged. In between the two line foci a blur circle is formed, called circle of least confusion. The plane containing the circle of least confusion often represents the best compromise image location in a system with astigmatism[5]. With Zernike polynomials, the astigmatism corresponds to the coefficients C_2^{-2} and C_2^2. The coefficient C_2^{-2} refers to the component of astigmatism with an axis either in the vertical or horizontal meridian and C_2^2 refers to oblique astigmatism with an axis either along the 45^0 or 135^0 meridians.

1.5.3 Coma

If the optical system is not perfectly symmetric about its optical axis, it suffers from off-axial aberration. Coma is one of the off-axial aberrations that occur mainly due to the shape

of the cornea[2]. If the eye suffers from coma, then an off-axial point object is imaged as a blurred surface with a head and a tail and looks like as a comet[48]. A refracting surface of the eye or any optical system is composed of many concentric thin surfaces called zones which extend from center to the outer edge. If each concentric zone of the surface has a different levels of magnification for the object then each zone of the surface produces its own comatic circle so the entire object is imaged as a comet[48] (Fig 1:8). With Zernike polynomials, the third order coma corresponds to the coefficients C_3^{-1} and C_3^1. The former is called vertical coma and the later is called horizontal coma. Coma is the significant aberration among the higher order aberrations.

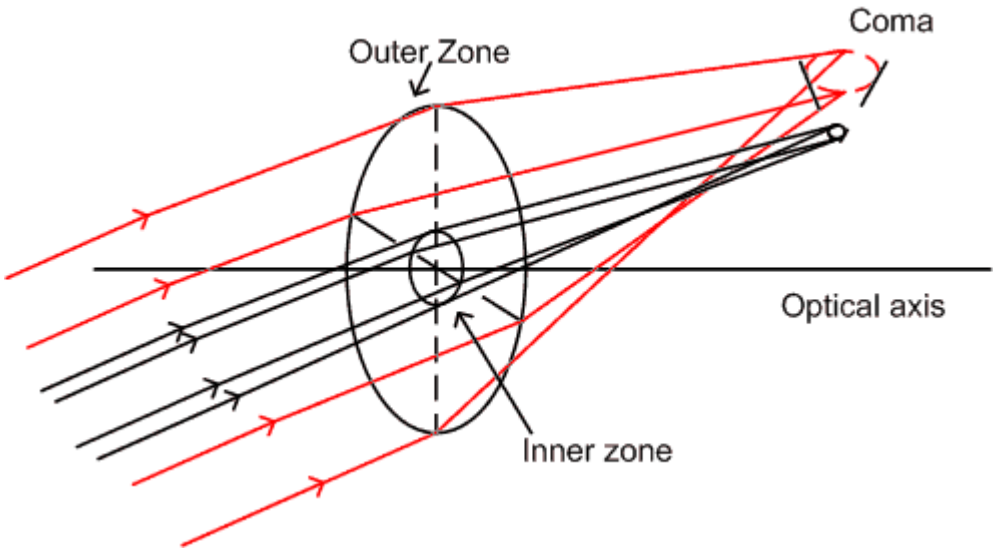

Figure 1:7 Schematic diagram showing the formation of coma

1.5.4 Trefoil

Trefoil is another prominent third order aberration which is also due to the asymmetry of the optical system about the optical axis. If the eye suffers from trefoil then an off-axial point

object is imaged as a blurred surface which resembles a blurred club of a playing card, giving it the name trefoil. In Zernike polynomials the third order trefoil corresponds to the coefficient C_3^{-3} and C_3^3. The former is called vertical trefoil and the later is called horizontal trefoil.

1.5.5 Spherical aberration

Spherical aberration is the only higher order aberration which depends upon an axial and off-axial object. As already discussed, the refracting surface of the eye or any optical surface is composed of many concentric circular zones. If each zone of the optical surface produces a different focal length for an object about the optical axis then the image of the point object appears as a blurred circle. The paraxial rays converge exactly at the paraxial focus but the peripheral rays focus either in front of or beyond the paraxial focus (Fig 1:9) depending upon either the excess or attenuation of the peripheral refractive power of the eye. The spherical aberration depends upon the shape of the optical system, position of the object and variation in the index of the refracting surface[48]. With Zernike polynomials, the fourth order spherical aberration corresponds to the coefficient C_4^0. Spherical aberration is the most prominent aberration in the fourth order aberration whose ocular effect is typically large and contributes to significant degradation in the quality of the retinal image.

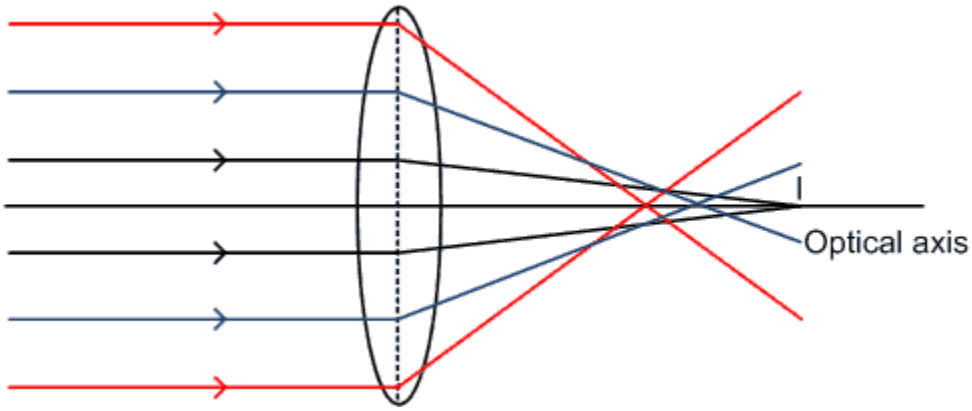

Figure 1:8 Schematic diagram showing the formation of positive spherical spherical aberration

1.6 Research aim

There are major anatomical and optical changes in the developing eyes of infants and children. From birth to puberty, the axial length increases in a somewhat asymptotic function[49]. The growth reflects a proportionately larger increase in the vitreal depth than the anterior chamber length[49]. The axial length increase is compensated by increases in the radii of curvature of both the cornea and lens[6]. The anterior chamber, the vitreous chamber continuously grows from birth to the adolescence. While much has been learned regarding the aberrations of the adult eye, considerably less is known regarding the pattern of aberrations found at various stages of development. This gap has reflected the difficulty of obtaining such measurements in young children who have limited spans of attention and co-operation and who do not tolerate the close working distances of traditional optical instruments. The major goal of this research is to obtain such measures in a large sample of pre school children.

Second order aberrations are best corrected by simple means like spectacle corrections, contact lenses or refractive surgery. In clinical terms they are simply called defocus and astigmatism. Wavefront technology allows the measurement and analysis of ocular aberrations beyond defocus and astigmatism[4]. Aberrations which can not be corrected by simple means are often referred to as higher order aberrations (HOA). In this thesis, an attempt is made to measure the higher order aberrations in terms of Zernike coefficients. This thesis is organized into seven chapters. The methods, instrumentations and study sample are described in the Second Chapter. The third chapter shows the correlations between the right and left eyes of the pediatric study participant. The development of higher order aberrations with respect to the age of the pre-school children is described in Chapter Four. The optical performance of the eye, in terms of Modulation Transfer Functions and Strehl ratios are compared in different visual acuity groups in Chapter Five. Ocular aberrations varying with respect to the magnitude of refractive error in a pre-school sample are demonstrated in Chapter Six. Chapter Seven provides a conclusion for this research and offers some suggestions for future work.

Chapter 2
Methods

2.1.1 Vision Screening and Follow-up Study

The ocular data for this thesis were taken from archived images that arose from a large scale vision screening and follow-up investigations conducted using a Welch Allyn® SureSight autorefractor. W.R. Bobier conducted the vision screening program at Oxford Country, in southeastern Ontario, Canada, with an area of 2032 km^2. The majority of population (88%) is primarily English speaking[50]. The screening was conducted from 2000 to 2006; pre-kindergarten registrants were assessed by public health nurses from the Oxford County Health Unit[50,51]. A research team was sent each spring to Oxford County to conduct a follow-up study on the pre-school children age ranges from 3 to 6 years. These investigations examined ocular patterns,[26,30,52,53] vision and literacy[54] and numerous technical reports provided to the Welch Allyn® Co. All investigations received ethics clearance from the Office of Research Ethics at the University of Waterloo. The working principles of the instruments used for the vision screening program are discussed below.

2.1.2 Welch Allyn® SureSight Autorefractor

The prototype Welch Allyn® SureSight wavefront sensor used in the vision screening is an objective hand-held autorefractor[55,56] that is designed primarily to screen refractive errors such as myopia, hyperopia and astigmatism. The instrument can automatically refract a child in less then 10 seconds at a test distance of 14 inches (35 cm). The objective autorefractor measures spheres from +6 to -4.5D and cylinders up to ±3.0D.[55,56] After each measurement,

refractive values (sphere, cylinder and axis) are displayed on the screen (Figure 2.1). After 5-8 trials the final printed result includes refractive values along with the associated reliability number. The reliability number depends on a number of parameters, including the quality of the images and the variability of the different readings. An arbitrary scale from 1 to 9 specifies the confidence levels of the measurement. A confidence level less than 4 is poor, 5 is marginal and 6 or greater is acceptable measure.[55-58] If the refractive error of a child exceeds the range of the instrument's measurement capabilities, then the printed result shows ±9.99 for sphere and +9.99 for cylinder. The instrument has two modes; the child mode is designed for assessing children aged six or younger whereas the adult mode is designed for over six years of age. The SureSight is marketed as portable, easy to use, and equally effective for children, disabled patients and those with a language barrier.[55,56]

The set up for the Welch Allyn® SureSight hand-held Auto-refractor is conventional; in which participants are seated comfortably in a chair. Examiners sit at eye level with the SureSight in their right hand. Examiners look through the peephole and align the crosshairs on the pupil of the child's test eye. The child is requested to view a test pattern with a blinking central red light surrounded by green lights. These lights are accompanied by high and low pitched beeps, which guide the examiners to find the appropriate test distance (35cm). For example, when the unit is too far away, low pitched beeps are heard and when the unit is too close, high pitched beeps are heard. When the instrument is moved close to the proper working distance (35cm) a steady low tone is heard and measurements are automatically taken. The auditory cues of the instrument also draw the attention of the

children. When the test on the first eye is complete, a “ta-dah” sound is heard which indicates that the measurement has been successfully taken[55-58].

©Welch Allyn Company

Figure 2:1 Welch Allyn Autorefractor

2.1.3 Cambridge Crowding Cards

The Cambridge Crowding Cards (CCC) test is designed to measure the visual acuity of pre-school children because it eliminates the need for children to name the letters.[60] Children match the letters on the card to those on a matching board. There are two methods of measuring the visual acuity; single letter display and multiple or ‘crowded’ letter display. The single letter display was used in Oxford Country vision screening program. The CCC test is carried out in a well illuminated room. Children sit at 3m distance with a matching

board on their lap. One eye is occluded and one optotype per level is presented to children starting from the 6/60 level and proceeding in a descending order. Children are asked to point to the letter on the matching board that matches the letter on the card. A pre-test is conducted to familiarize children with the test procedure in order to minimize errors. The optotypes are continuously presented in a descending order until an error is made. Then the investigator goes one level up and presents two optotypes per level. If 2 are correctly matched, then the investigator proceeds to the smaller letters. If only 1 out of 2 letters are correctly matched then a third letter is presented. The passing criterion is 2 out of 3 correct letters.[60]

2.2 Study sample

For this thesis project, the anonymized archived records were retrieved from the Oxford study between 2000 to 2006. These records included cyclopledged refractions from Welch Allyn® SureSight Autorefractor, retinoscopy measurements and CCC visual acuities. This study was exclusively related to the data and statistical analysis of Hartmann-Shack images. Images taken from refractive assessments of a preschool sample using a prototype of the Welch Allyn® SureSight were reanalyzed in order to allow measures of ocular aberrations in addition to refractive error. More than 3000 Hartmann-Shack images from 543 children were reviewed over the dates from 2000 to 2006. We selected 834 images of 436 children (right eye 436 and left eye 399). The remaining 107 children were excluded from this study because they did not meet the selection criterion. Images were selected according to the confidence limit of the instrument, pupil dilation, pupil diameter, and attention and co-operation of the child during the examination. Only cyclopledged images with confidence limit greater than 6 were eligible for this study. The average pupil diameter of the 543

children was 5.6 ±0.82 mm (range 3.3 to 7 mm). Only images with pupil diameter greater than 5 mm were selected for this study. Ninety two children were excluded due to this criterion. Zernike coefficients were calculated using the reconstruction algorithms. If the reconstruction algorithm calculates too many Zernike coefficients compared to the number of lenslets then the method becomes inaccurate and causes unpredictable error[46]. Our software calculates Zernike coefficients up to the tenth order which can be measured reliably only if the image contains at least 65 sampling points (i.e. number of lenslets). So Hartmann-Shack images with less than 65 spots were excluded from this study. Images from improperly dilated eyes were also excluded from this study (2 children). Children are very sensitive and frequently loose their attention. Some of the children had a short span of attention for the target; they were also excluded (6 children). Some of the children were very shy and did not co-operate for the test (7 children). These images were not included for this study. Mean Zernike coefficients of at most three images were taken if more than one image of the same subject was equally good. The ages of the children ranged from 3 to 6 years; 37.5% were 3 years, 42.15% were 4 years, 12.25% were 5 years and 8.1% were 6 years. The population showed a mean hyperopic spherical equivalent of 1.19± 0.63D, a mean with-the-rule astigmatism of 0.058 ± 0.22D and a mean oblique astigmatism of 0.033 ±0.13D. Visual acuity varied from 6/6 to 6/18; 72.7% of eyes had 6/6 VA, 23.7% of the eyes had 6/9 VA, and 3.6% of eye had 6/12 level of visual acuity.

2.3 Instrument calibration

The Welch Allyn® SureSight wavefront sensor is based on the principle of Hartmann-Shack wavefront analyzer[56], exploiting Scheiner's principle. Light from the illuminated

source situated at the top of the instrument is incident on the eye of the patient and focused at the retina. The light reflected from the retina passes through a series of mirrors and is finally received by the Hartmann-Shack wavefront sensor (lenslet array)[56]. Lenslet arrays converge the light and hence a spot pattern of light is formed on the CCD camera (Fig 2.2). Finally the spot pattern is translated into the spheres, cylinder and axis values[56].

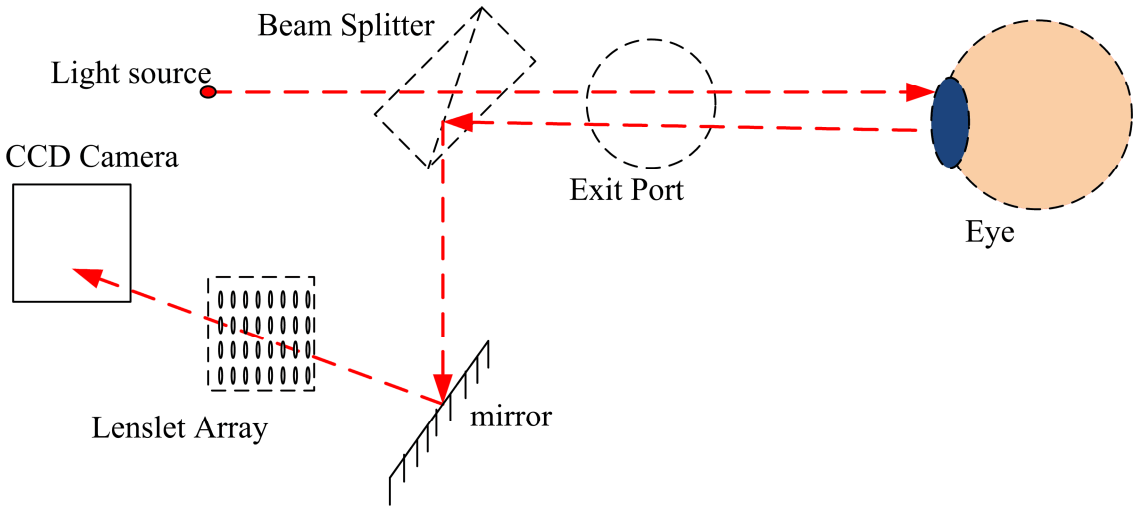

Figure 2:2 Schematic diagram of Welch Allyn® Suresight wavefront sensor

The optical design of Welch Allyn® SureSight Autorefractor is propriatory and hence confidential. Confidential investigations in concert with Welch Allyn® were undertaken in order that the unique Hartmann-Shack design for this instrument could be determined and then expanded in order to measure aberrations. To calibrate this instrument, the reference grid was recalculated using input image characteristics such as the average centroid spacing across the pupil in both x and y directions (with axis determined by lenslet array). Additional corrections based upon the pupil size, pupil location with respect to the CCD and individual

lenslet fabrication errors were implemented. The MATLAB code proposed by Thibos et al.[61] that follows the standard for reporting the optical aberrations of the eye was the basis of code written specifically for this study. Modification was required to suit the specific needs of the SureSight instrument such as the size, spacing and focal length of the lenslet. This software was compiled and extensively modified to suit the specific needs of this project by Andre Fleck[62] in our laboratory here at the University of Waterloo. For validation of this software, measurements of model eyes with known aberrations were compared with Alcon and Zeiss aberrometers and lower order aberrations were also compared against retinoscopy measurements from the vision screenings.

Chapter 3
Symmetry in Ocular Aberration between Fellow Eyes

3.1 Introduction

The visual process starts with the optical imaging followed by transduction of light into the electrical impulses and finally completes with the transmission of electrical impulses to the brain. The quality of vision depends upon optical aberrations, cone directionality, photoreceptor topography, neural noise and the performance of optical nerves. All the above factors differ considerably from individual to individual.[7,41,63,64,65] Several studies observed inter-subject variability in the optical system either in terms of the RMS value,[41] or the point spread function, modulation transfer function, and Strehl ratio.[66] It is of interest to observe whether these metrics correlate between eyes in the same subject, or if in contrast, these metrics develop differently between the left and right eyes of the same individual.

The visual performance of human infants improves considerably after birth due to the development of optical structures of the eye[7]. The ocular growth involves both the anatomical and optical changes such as increase in the axial length, flattening of the corneal curvature, and thickening the crystalline lens. A given eye may develop differently from its fellow eye. Anisometropia is the difference in refractive state between the eyes that occurs if either the refractive power or the axial length of one eye does not correlate with its fellow eye. Hyperopic anisometropia both with and without astigmatism, has been reported to be more common than other types of anisometropia[67]. De Vries[67] reported a 4.7% prevalence of anisometropia of at least 2D in children. Hirch[68] found more than 1D of anisometropia in

2.5% of children entering school. Larsson and Holmstrom[69] studied the development of anisometropia in preterm children during the first 10 years of life and observed no change from 6 month to 2½ years of age, but an increase between 2½ and 10 years. The anisometropia developed in some children and disappeared in others; however, the overall prevalence remained unchanged. Similar results was observed by Ingram and Barr[70] where 7 anisometropic children at 1 year were not anisometropic at 3½ of age while 8 children, who were not anisometropic at 1 year, were anisometropic at 3½ years of age. Abrahamsson, Fabian and Sjostrand[71] observed 19 out of 33 children with anisometropia at age 1 year were not anisometropic at 3 while 14 other children, who were non-anisometric at the age of 1 year, became anisometropic by age 3. In this study, anisometropia is defined in terms of the difference in spherical equivalent between the eyes. Theoretically, different amounts of ocular accommodation are required if the refractive state of the eye changes[5].

Some studies[72-76] in young adult and aged eyes revealed a mirror symmetry in higher order aberrations between the left and right eyes. However, there has not been any study conducted to examine the symmetry in ocular aberration between the eyes of the children to date. It is of interest to examine ocular symmetry when the optical components of the eyes are developing. So the main purpose of this chapter was to observe the symmetry of ocular higher order aberrations between right and left eyes in a pre-school group.

3.2 Methods

3.2.1 Subjects

Total of 834 images of 436 children (right eye 436 and left eye 399) were reliable for this analysis; however, in this chapter, both right and left eyes images of a subject were needed. Only 796 images of 398 subjects (mean age 3.93 years ±0.93STD, range 3 to 6 years) met this criterion. The population showed a mean (± STD) spherical equivalent of 1.176±0.60D (range -1.5D to +3.2 D), a mean with-the-rule astigmatism of 0.058±0.22D (range -0.72D to 1.38D) and a mean oblique astigmatism of 0.01±0.14D (range -0.78D to 0.88D). The visual acuity of the subject varied from 6/6 to 6/18. Detailed demographic descriptions of the participants included in this study are described below in Table 3.1.

Table 3:1 Demographic description of subjects included in this study

Eyes	N	Sp. Eq.	J0	J45
Right	398	1.17±0.62D	0.06±0.22D	-0.01±0.14D
Left	398	1.19±0.57D	0.055±0.22D	0.03±0.14D
Total	796	1.176±0.60D	0.058±0.22D	0.01±0.14D

3.2.2 Data analysis

Zernike coefficients were calculated for a pupil size of 5 mm. Date were calculated using SPSS (version 17.0). A paired t-test was used to find the statistical significance in the mean values of the higher order aberrations between the right and left eyes. A Pearson correlation coefficient was calculated to examine the association between the left and right eyes. In this

chapter: a) higher order aberrations from 3rd to 8th order; b) total coma; c) total trefoil; d) total spherical aberration; e) total third order aberration; f) total fourth order aberration; g) total fifth order aberration; h) total sixth order aberration; i) total seventh order aberration; j) total eight order aberration, were analyzed. The Bonferroni correction for multiple tests of correlation was also performed to find the correlation of each Zernike term from the third to the eighth orders (39 Zernike terms). Probability of less than ($p<0.05/39$) was considered as significantly correlated to maintain the overall significance level of 5% ($p<0.05$).

3.3 Results

In this sample, 20 out of 21 Zernike modes with even symmetry were positively correlated and 14 out of 18 Zernike modes with odd symmetry were negatively correlated. The correlation was significant ($p<0.05$) for 13 out of 21 Zernike modes with even symmetry and for 7 out of 18 Zernike modes with odd symmetry showing the moderate mirror symmetry between the right and left eyes of the children (Table 3.2).

The mean (± standard deviation) RMS values of total higher order aberration (HOA) from 3rd to 8th order were $0.1828\pm0.0645\,\mu m$ and $0.1886\pm0.0717\,\mu m$ for right and left eyes, respectively (Table 3.3). Total HOA varied from individual to individual, and the range of HOA in our population was from $0.0588\,\mu m$ to $0.5786\,\mu m$. The paired t-test showed no significant difference ($p=0.094$) in total higher order aberrations between the right and left eyes (Fig 3.1).

Table 3:2 Descriptive statistics of different Zernike terms up to the 8th order between the right and left eyes

Zernike terms	Left eye Mean± STD	Right eye Mean± STD	Pair t-test	Correlation coefficient	Sig cor P<0.0013
C^{-3}_3	0.0094±0.0668	0.0152±0.0641	0.079	0.493	0.001
C^{-1}_3	0.0150±0.1076	0.0172±0.0986	0.607	0.651	0.001
C^{1}_3	-0.0144±0.0803	0.0331±0.0742	0.000	-0.226	0.001
C^{3}_3	-0.0099±0.0681	0.0062±0.0666	0.004	-0.373	0.001
C^{-4}_4	-0.0043±0.0270	0.0040±0.0260	0.000	-0.071	0.158
C^{-2}_4	0.0014±0.0254	-0.0038±0.0237	0.005	-0.112	0.025
C^{0}_4	-0.0047±0.0658	-0.0049±0.0640	0.943	0.798	0.001
C^{2}_4	0.0142±0.0376	0.0166±0.0383	0.249	0.392	0.001
C^{4}_4	-0.0071±0.0354	-0.0039±0.0314	0.071	0.443	0.001
C^{-5}_5	-0.0032±0.0178	-0.0041±0.0166	0.385	0.200	0.001
C^{-3}_5	-0.0064±0.0185	-0.0070±0.0181	0.543	0.361	0.001
C^{-1}_5	0.0100±0.0249	0.0108±0.0234	0.513	0.437	0.001
C^{1}_5	0.0011±0.0160	0.0005±0.0159	0.613	-0.143	0.004
C^{3}_5	-0.0055±0.0157	0.0030±0.0134	0.000	-0.004	0.934
C^{5}_5	0.0022±0.0163	0.0006±0.0150	0.189	-0.089	0.075
C^{-6}_6	0.0009±0.0110	-0.0002±0.0110	0.136	-0.030	0.552
C^{-4}_6	0.0006±0.0093	-0.0000±0.0084	0.297	-0.054	0.285
C^{-2}_6	-0.0018±0.0117	0.0021±0.0117	0.000	-0.126	0.012
C^{0}_6	-0.0054±0.0171	-0.0075±0.0164	0.027	0.383	0.001

C^{2}_{6}	0.0015±0.0125	0.0024±0.0127	0.247	0.166	0.001
C^{4}_{6}	-0.0008±0.0101	-0.0026±0.0099	0.007	0.131	0.009
C^{6}_{6}	-0.0015±0.0121	-0.0002±0.0118	0.126	0.033	0.516
C^{-7}_{7}	-0.0011±0.0087	-0.0018±0.0091	0.220	0.154	0.002
C^{-5}_{7}	0.0005±0.0071	0.0015±0.0069	0.036	0.073	0.145
C^{-3}_{7}	-0.0032±0.0085	-0.0034±0.0075	0.619	0.231	0.001
C^{-1}_{7}	-0.0032±0.0115	-0.0030±0.0103	0.786	0.256	0.001
C^{1}_{7}	0.0014±0.0099	-0.0001±0.0091	0.016	0.027	0.594
C^{3}_{7}	-0.0003±0.0067	0.0003±0.0067	0.165	-0.043	0.388
C^{5}_{7}	0.0007±0.0065	-0.0001±0.0065	0.066	0.014	0.787
C^{7}_{7}	-0.0007±0.0084	0.0006±0.0086	0.015	0.056	0.262
C^{-8}_{8}	0.0001±0.0070	-0.0013±0.0079	0.003	0.133	0.008
C^{-6}_{8}	-0.0003±0.0055	0.0001±0.0050	0.135	0.064	0.205
C^{-4}_{8}	0.0001±0.0049	-0.0005±0.0050	0.056	-0.080	0.110
C^{-2}_{8}	0.0002±0.0056	0.0000±0.0055	0.567	-0.102	0.042
C^{0}_{8}	0.0060±0.0076	0.0053±0.0077	0.100	0.411	0.001
C^{2}_{8}	-0.0005±0.0060	-0.0006±0.0060	0.903	0.067	0.181
C^{4}_{8}	0.0008±0.0056	0.0012±0.0054	0.326	-0.018	0.717
C^{6}_{8}	0.0001±0.0056	-0.0000±0.0060	0.604	0.088	0.081
C^{8}_{8}	0.0002±0.0073	-0.0006±0.0076	0.098	0.036	0.469

Total coma (i.e. RMS of C^{-1}_3, C^{1}_3, C^{-1}_5, C^{1}_5, C^{-1}_7 and C^{1}_7) were 0.1174±0.0625 μm and 0.1212±0.0705 μm (Table 3.3) for right and left eyes, respectively (range 0.0098 μm to 0.4058 μm). The total coma was the largest higher order aberration in this sample followed by total trefoil and total spherical aberration. No significant difference (p=0.283) in mean RMS values of the total coma (TC) was found between the right and left eyes (Fig 3.1).

The total trefoil was the second most prominent higher order aberrations term. The mean RMS values of the total trefoil (TT) (i.e. RMS of C^{-3}_3, C^{3}_3, C^{-3}_5, C^{3}_5, C^{-3}_7 and C^{3}_7) were 0.0860±0.0457 μm and 0.0887±0.0469 μm (Table 3.3) for right and left eyes, respectively (range 0.0115 μm to 0.3988 μm). The paired t-test showed no significant difference (p=0.317) in the total trefoil between the right and left eyes (Fig 3.1). Similarly, the mean RMS values (i.e. RMS of C^{0}_4, C^{0}_6 and C^{0}_8) of the total spherical aberration (TSA) were 0.0556±0.0380 μm and 0.0569±0.0391 μm for left and right eyes, respectively (range 0.0032 μm to 0.2327 μm) (Table 3.3) and no significant difference (p=0.445) was observed between them (Fig 3.1).

The mean (± standard deviation) RMS values of the third order aberration were 0.1452±0.0656 μm and 0.1501±0.0720 μm (Table 3.3) for the right and left eyes, respectively (range 0.0193 to 0.5576 μm). The third order Zernike coefficients completely followed the mirror symmetry between the left and right eyes. All the 4 Zernike coefficients of the 3rd order aberration were significantly correlated (p<0.001) with their fellow eyes. No significant interocular difference (Paired t-test p=0.173) was found in the RMS mean values of the third order aberrations (Fig 3.2).

Table 3:2 Descriptive statistics of RMS values of higher order aberrations of 796 eyes

Aberration	Right eye Mean ± STD	Left eye Mean ± STD	Pair t-test	Correlation Coefficient	Sig cor p<0.05
HOA	0.1828±0.0645	0.1886±0.0717	0.094	0.503	0.001
TC	0.1174±0.0625	0.1212±0.0705	0.283	0.467	0.001
TT	0.0860±0.0457	0.0887±0.0469	0.317	0.345	0.001
TSA	0.0556±0.0380	0.0569±0.0391	0.445	0.608	0.001
Third	0.1452±0.0656	0.1501±0.0720	0.173	0.473	0.001
Fourth	0.0819±0.0377	0.0847±0.0385	0.147	0.499	0.001
Fifth	0.0409±0.0181	0.0438±0.0177	0.008	0.256	0.001
Sixth	0.0305±0.0119	0.0302±0.0132	0.663	0.342	0.001
Seventh	0.0219±0.0093	0.0226±0.0101	0.243	0.287	0.001
Eighth	0.0185±0.0075	0.0183±0.0071	0.673	0.271	0.001

The mean RMS values of the total fourth order aberration were $0.0819\pm0.0377\,\mu m$ and $0.0847\pm0.0385\,\mu m$ (Table 3.3) for right and left eyes, respectively (range 0.0152 to $0.2658\,\mu m$). Among the Zernike terms from 3rd to 8th order C^0_4 was the most significantly correlated term ($r = 0.798$, $p<0.001$). Three out of 5 fourth order Zernike terms were significantly correlated with their fellow eye; however, C^{-4}_4 and C^{-2}_4 were not significantly correlated. The paired t-test showed no significant difference ($p=0.147$) in the RMS values of the 4th order aberration between the right and left eyes (Fig 3.2).

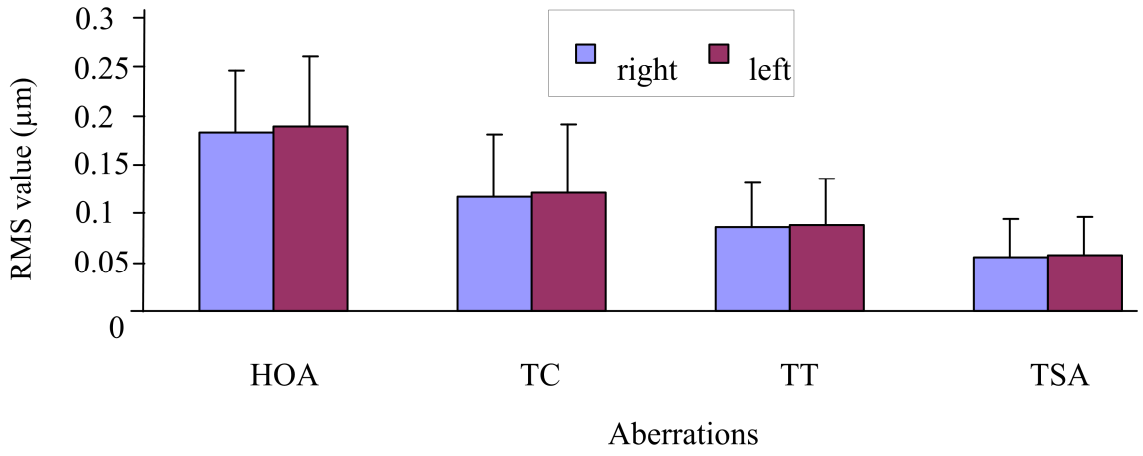

Figure 3:1 Mean values of total higher order aberration (HOA), total coma (TC), total Trefoil (TT) and total spherical aberration (TSA) between the right and left eyes. No significant differences ($p<0.05$) in higher order aberrations were observed. The error bar showed one standard deviation.

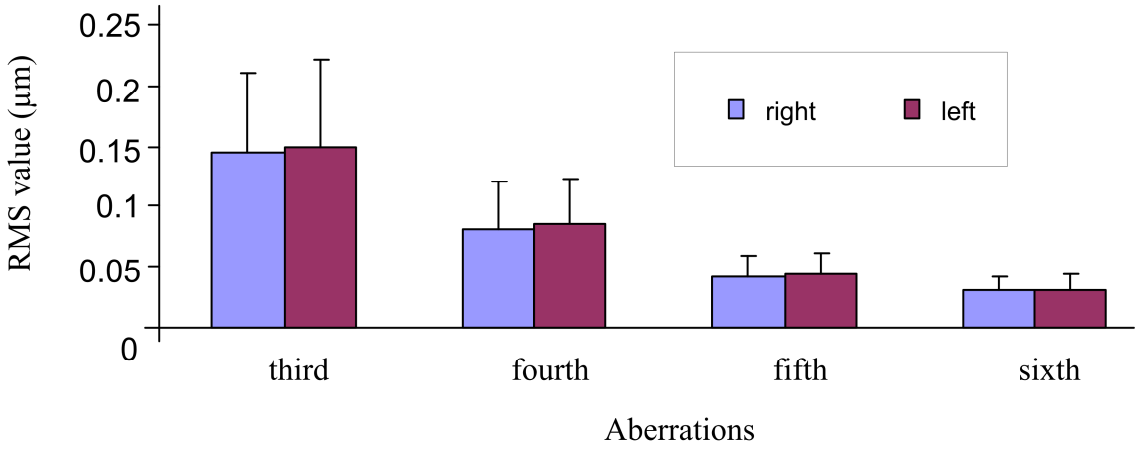

Figure 3:2 Mean values of total third, fourth, fifth and sixth order aberrations. No significant difference ($p<0.05$) in higher order aberrations were observed except for fifth order aberrations. The error bar showed one standard deviation.

The mean RMS values of the total fifth order aberration for the right and left eyes were 0.0409±0.0181 μm and 0.0438±0.0177 μm (Table 3.3), respectively (range 0.0088 μm to 0.1519 μm). Three (C^{-5}_5, C^{-3}_5 and C^{-1}_5) out of 6 Zernike modes for the fifth order aberration were significantly correlated ($p<0.001$) with their fellow eye, whereas the other three (C^{1}_5, C^{3}_5 and C^{5}_5) terms were not significantly correlated. A significant difference ($p=0.008$) in RMS values of the fifth order aberration was found between the right and left eyes (Fig 3.2).

The mean (± standard deviation) RMS values of the sixth order aberration were 0.0305±0.0119 μm and 0.0302±0.0132 μm (Table 3.3) for right and left eye, respectively (range 0.0078 μm to 0.1132 μm). Two out of 7 Zernike coefficients (C^{0}_6 and C^{2}_6) for the sixth order aberration were significantly correlated ($p<0.001$) with their fellow eyes. No significant difference (Paired t-test $p=0.663$) in the RMS values of the sixth order aberration was found between the right and left eyes (Fig 3.2).

The mean RMS values of the total seventh order aberration for the right and left eyes were 0.0219±0.0093 μm and 0.0226±0.0101 μm, respectively (range 0.0040 μm to 0.0776 μm) (Table 3.3). Two (C^{-3}_7 and C^{-1}_7) out of 8 seventh order Zernike terms were significantly correlated with their fellow eye. The paired t-test showed no significant difference ($p=0.243$) in the RMS values of the seventh order aberration between the right and left eyes. The mean RMS values of the total eighth order aberration were 0.0185±0.0075 μm and 0.0183±0.0071 μm (Table 3.3) for the right and left eyes, respectively (range 0.0036 μm to 0.0581 μm). Only one (C^{0}_8) out of 9 Zernike terms of the eighth order aberration were

significantly correlated ($p<0.001$) with their fellow eye. No significant difference ($p=0.673$) in mean values of the eighth order aberrations were found between the right and left eyes.

The Pearson correlation coefficients between the eyes showed significant correlations in RMS values for total higher order aberrations ($r=0.503$, $p<0.01$) (Fig 3.3), total coma ($r = 0.503$, $p<0.01$) (Fig 3.4), total trefoil ($r =0.345$, $p<0.01$) (Fig 3.5), total spherical aberration ($r= 0.608$, $p<0.01$) (Fig 3.6), total third order aberration ($r = 0.473$, $p<0.01$) (Fig 3.7), total fourth order aberration ($r=0.499$, $p<0.01$) (Fig 3.8), total fifth order aberration ($r = 0.256$, $p<0.001$), total sixth order aberration ($r = 0.342$, $p<0.001$), total seventh order aberration ($r=0.287$ ($p<0.001$) and the total eighth order aberration ($r = 0.271$, $p<0.001$).

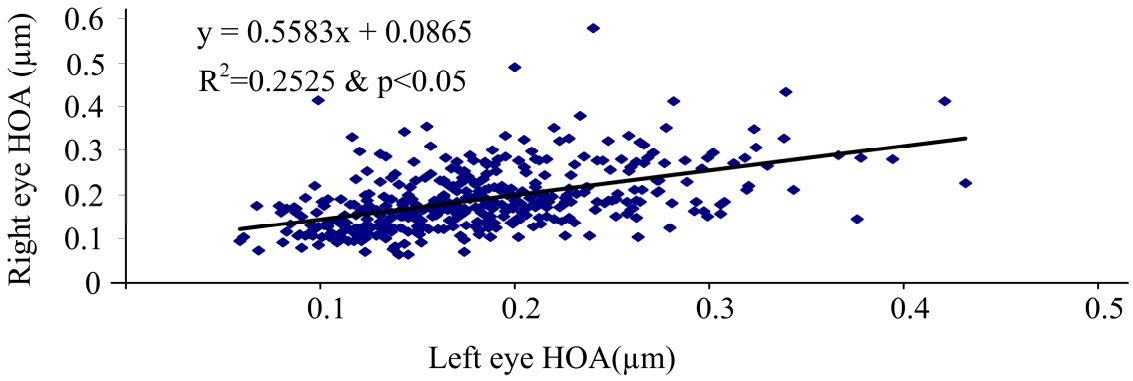

Figure 3:3 Correlation of total higher order aberrations (HOA) between the right and left eyes. Significant correlation ($p<0.05$) was found between the eyes.

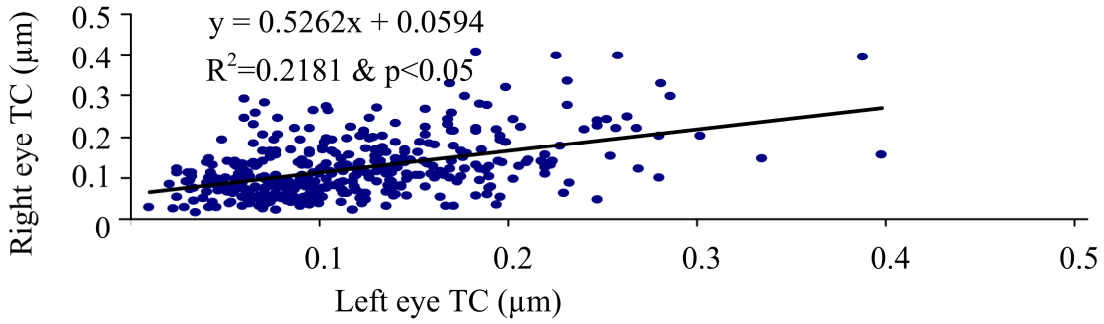

Figure 3:4 Significant correlation ($p<0.05$) was found in terms of total coma (TC) between the eyes.

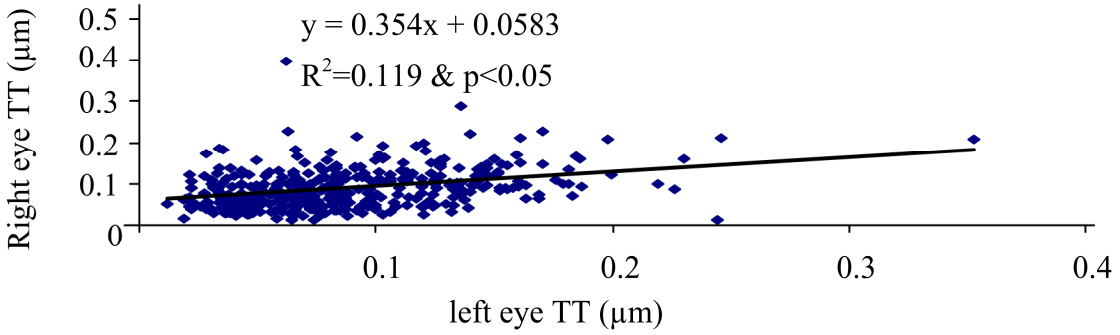

Figure 3:5 Significant correlation ($p<0.05$) was found in terms of total trefoil (TT) between the eyes.

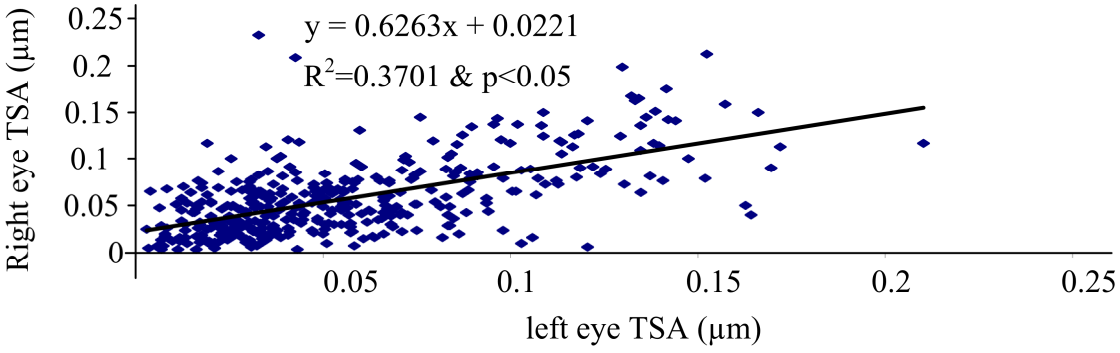

Figure 3:6 Significant correlation ($p<0.05$) was found in terms of total spherical aberrations (TSA) between the eyes.

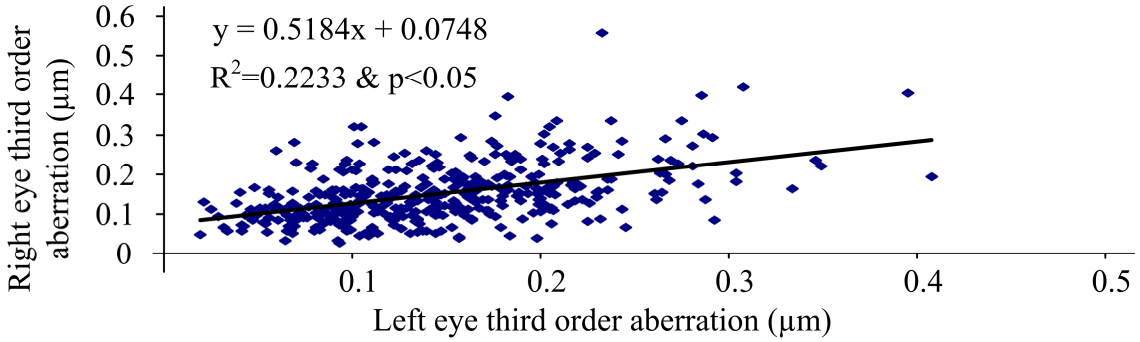

Figure 3:7. Significant correlation ($p<0.05$) in total third order aberration was found between the eyes.

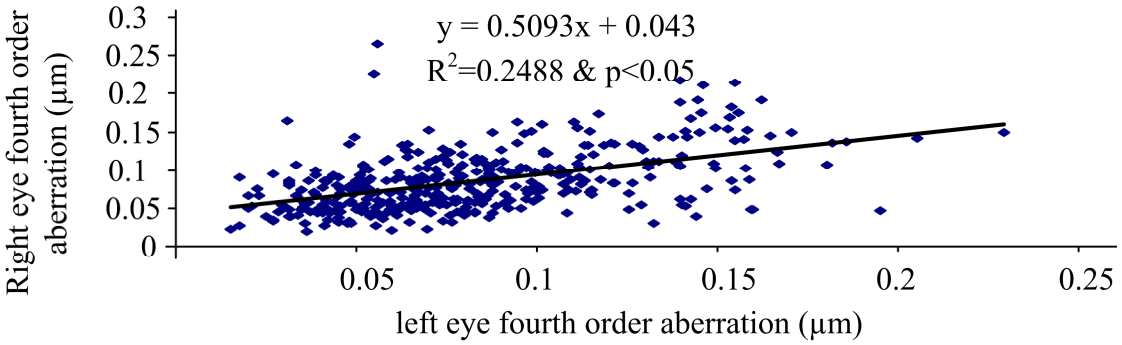

Figure 3:8 Significant correlation ($p<0.05$) in total fourth order aberration was found between the eyes.

3.4 Discussion

The mean (± standard deviation) RMS value of total HOA from 3rd to 8th order of total 796 eyes was $0.186\pm0.068\,\mu m$. The finding was comparable to that of Carkeet et al[77]. The ocular HOA varied greatly from subject to subject in this sample. The greatest variation was found in the total third order aberrations with the mean STD of $0.072\,\mu m$. Mirror symmetry between the left and right eyes requires that the wavefront of the left eye W(x, y) be identical to the wavefront of the right eye W(-x, y) for Zernike modes with even symmetry about the y-axis, it also demands a negative sign for Zernike modes with odd symmetry about the y-

axis[72]. A positive correlation was expected for even symmetry and a negative correlation was expected for odd symmetry. That is, expected positive correlation for C^{-3}_{3}, $C^{-1}_{3,}$ C^{0}_{4}, C^{2}_{4}, $C^{4}_{4,}$ C^{-5}_{5}, C^{-3}_{5}, $C^{-1}_{5,}$ $C^{0}_{6,}$ $C^{2}_{6,}$ C^{4}_{6}, $C^{6}_{6,}$ $C^{-7}_{7,}$ C^{-5}_{7}, C^{-3}_{7}, $C^{-1}_{7,}$ $C^{0}_{8,}$ $C^{2}_{8,}$ C^{4}_{8}, C^{6}_{8} and C^{8}_{8} and negative correlation for remaining modes C^{1}_{3}, $C^{3}_{3,}$ C^{-4}_{4}, $C^{-2}_{4,}$ C^{1}_{5}, C^{3}_{5}, $C^{5}_{5,}$ $C^{-6}_{6,}$ C^{-4}_{6}, $C^{-2}_{6,}$ C^{1}_{7}, C^{3}_{7}, C^{5}_{7}, $C^{7}_{7,}$ C^{-8}_{8}, C^{-6}_{8}, C^{-4}_{8} and C^{-2}_{8}. These findings showed moderate mirror symmetry between the fellow eyes. Twenty out of 39 Zernike terms were significantly correlated (Bonferroni correction $p<0.001$) between the eyes. Among them, the 4th order spherical aberration term (C^{0}_{4}) was the strongest correlated term ($r=0.798$), followed by vertical coma ($r=0.651$) and vertical trefoil ($r=0.493$).

These findings agree with previous studies[72-76] conducted on adult (subjects aged from 20 to 80 years), that showed a mirror symmetry in Zernike modes between left and right eyes. For example, Wang and Koch[72] performed correlation analysis between the left and right eyes of 227 subjects (mean age 41 years ±10SD) with a wide range of spherical equivalents (-11.56 to 7.60D) and found the mirror symmetry between the eyes. They carried out correlation analysis of the Zernike modes from the 3rd to 6th order and found that 13 out of 22 Zernike terms were significantly correlated (Bonferroni correction $p<0.002$) between the right and left eyes. A similar result was found by Porter el al[74], who found 13 out of 18 Zernike terms were significantly correlated ($p<0.01$) between the right and left eyes in their subject population aged from 21 to 65 years. However, Marcos and Burns[63] were unable to find mirror symmetry in higher order aberrations between right and left eyes. The wavefront aberration in terms of total RMS values were comparable between the eyes of 8 out of 12

subjects but only eyes of 4 out of 12 subjects had mirror symmetry in their study sample. This might be due to the less number of subjects.

The findings of this chapter were slightly different from that reported by Wang and Koch[72]. There were significant correlations ($p<0.001$) for the third order Zernike terms (C^1_3 and C^3_3) as well between the right and left eyes as reported by Porter et al[74] unlike that reported by Wang and Koch[72]. The study sample of Wang and Koch[72] consisted of people in the age range 20-71 years. The ocular symmetry between the eyes of adults might be different from that of the growing eyes of children. The subtle differences in ocular HOA between the eyes of children may be caused by the uncorrelated ocular growth such as changes in axial length, an increase in corneal curvature, thickening crystalline lens and change in the refractive index of the eye. Variation of ocular HOA with the axial length or size of the eyes was beyond the scope of this research but we expect that unequal growth in axial length and the eye's size could be the possible source of difference in ocular HOA between the fellow eyes.

In this study sample, 63.5% of children had the same level of visual acuity (6/6) in their eyes. Fifteen percent showed the same 6/9 level of visual acuity. A small portion (1.5%) showed the same 6/12 level of VA; however, a large portion of the population (16%) showed 6/6 VA in one eye and 6/9 level of VA in the corresponding fellow eye. Two percent of the children had 6/9 VA in one eye and 6/12 VA in the other eye. The remaining 2% of the sample had different levels of VA between their fellow eyes. In total, 20% of the eyes of this study group had different levels of visual acuity. The difference in visual acuity might cause different levels of HOA between the fellow eyes since chapter 5 of this thesis shows lower

but not significant amounts of higher order aberration for better visual acuity groups. Recent research also revealed that there is no significant difference in HOA between those with supernormal vision (i.e. VA> 20/15) and myopies[78,79].

As the eye grows, the optical power of the crystalline lens and cornea must tightly coordinate with the increase in the axial length of the eye. Differences in refractive power of the fellow eyes causes anisometropia and which may further contribute to different levels of higher order aberrations between the eyes. In this sample, 83% of the children had less than 0.5D of anisometropia, 15.5% had between 0.5D and 1D of anisometropia, and 1.5% had greater than 1D of anisometropia. Anisometropia may be a possible cause of not having perfect symmetry between the eyes. It is difficult to find studies relating the association between anisometropia and aberrations. Few studies have been done to observe the association between anisometropia and refractive errors. For example, Qin, Margrain and To[80] showed a positive correlation between the level of anisometropia and spherical ametropia, astigmatism and age.

In summary, moderate mirror symmetry was found in the eyes of growing children. Although, mean values of higher order aberrations were slightly different between the eyes, no significant differences in higher order aberrations were found. Higher order aberrations were significantly correlated between the eyes.

Chapter 4
Ocular Aberration and Age in Pre-school Children

4.1 Introduction

Visual performance improves with the improvement in the optical and neural components of the eye. Both components develop with age; however, herein we mainly study the optical components change with age. As discussed in the previous chapter, the average child is born with hyperopia and the degree of refractive error changes from hyperopia through emmetropia to myopia with age[13]. Several studies have been conducted to assess the association between age and ocular aberrations[81-89]. Significantly larger higher order wavefront aberrations have been reported in aged eyes compared to young adult eyes in several studies[66,81,86]. Studies have observed a weak but significant correlation between higher order aberrations and age in their subjects aged from 20 to 70 years.[82-85] For example, McLellan et al.[82] measured the monochromatic wavefront aberration of 38 subjects, aged 22.9 to 64.5 years, using a spatially resolved refractometer. They found significant correlations ($r=0.33$, $p=0.042$) with age for the total higher order aberrations from the third to the seventh order. The image quality computed in terms of modulation transfer function (MTF) was also degraded with age. Guirao et al.[66] and Artal et al.[81] also observed a significant loss of image quality in terms of MTF with age. Others studies[87, 88] conducted on young adult and aged people have reported no significant difference in total higher order aberrations between different age groups. Calver et al.[88] used crossed-cylinder aberroscopes and studied the effect of aging on the monochromatic aberration of the human eyes and observed no significant different in RMS values of higher order aberrations between the

young (n= 15, mean age 24.2±3 years) and old people (n= 15, mean age 68 ±5 years). The contrast sensitivity function declined with age but they concluded that this decline was not due to the increase in wavefront aberration but rather it was due to the other factors such as the changes in neural transfer function, light absorption or light scattering.

While much is known regarding the association between ocular aberrations and age in adults, it is of interest to observe the association between age and ocular aberration in the pre-school population where hyperopia gradually reduces with age. So the main purpose of this chapter is to study the development of higher order aberrations from 3 years to 6 years.

4.2 Methods

4.2.1 Subjects

All 834 images of 436 children (right eye 436 and left eye 399) were suitable for this study; however, the third chapter of this thesis shows significant correlation in higher order aberrations between the eyes. So, only right eyes of 436 children were included in this chapter (mean age 3.877± 0.898 years, range 3 to 6 years). The sample showed a mean spherical equivalent of 1.19± 0.63D, a mean with-the-rule astigmatism of 0.058 ± 0.22D and a mean oblique astigmatism of 0.033 ±0.13D. The visual acuity of the subjects varied from 6/6 to 6/18. The complete demographic summary of subjects included in this chapter is shown in Table 4.1.

4.2.2 Data analysis

Zernike coefficients calculated for a pupil size of 5 mm were used to study the development of higher order aberration with age. Higher order aberrations were presented as

root-mean-square (RMS) values. In this chapter, an attempt was made to calculate: a) root mean square (RMS) values of higher order aberrations from 3rd to 8th orders; b) total coma (RMS of C_3^1, C_3^{-1}, C_5^{-1} C_5^1 and C_7^1, C_7^{-1}); c) total trefoil (RMS of C_3^3, C_3^{-3}, C_5^3, C_5^{-3} and C_7^3, C_7^{-3}); d) total spherical aberration (RMS of C_4^0, C_6^0, C_8^0). Total third, fourth, fifth, sixth, seventh and the eighth order aberrations were also analyzed. Data were analyzed using SPSS (version 17.0). Multivariate analysis of variance was used to examine the effect of age on higher order aberrations. Hotelling's trace method was used to calculate the significance level and it was fixed at 0.05 levels. If multivariate analysis of variance showed a significant difference in higher order aberrations between different age groups, then Bonferonni post-hoc test was carried out to test multiple comparisons. Finally, Pearson correlation coefficients were calculated to examine the correlation between higher order aberrations and age.

Table 4:1 Demographic summary of subjects included in this chapter's study

Age	n	Sp. Eq. (Mean ± SD)	J0 (Mean ± SD)	J45 (Mean ± SD)
3	172	1.30±0.61D	0.036±0.23D	0.039±0.14D
4	176	1.16±0.66D	0.078±0.23D	0.031±0.15D
5	50	1.05±0.62D	0.045±0.15D	0.016±0.10D
6	38	1.02±0.49D	0.088±0.17D	0.043±0.09D
total	436	1.19±0.63D	0.058±0.22D	0.033±0.13D

4.3 Results

The right eyes of 436 young pre-school children were studied. In this sample, refractive error significantly decreased (p=0.011) with age (one-way ANOVA). Moreover, a significant

negative correlation was observed between age and refractive error ($r=-0.154$, $p<0.01$). With-the-rule astigmatism (J_0) was not significantly different among 3, 4, 5 and 6 year age groups. No significant correlation ($r=0.063$, $p=0.193$) was observed between with-the-rule astigmatism and age. Similarly, oblique astigmatism was not significantly different ($p=0.708$) among ages and no significant correlation ($r=-0.02$, $p=0.683$) was observed between oblique astigmatism and age.

Ocular aberration was found to vary from subject to subject in our sample. The average distribution of Zernike coefficients along with standard deviation in different modes are shown in Fig 4.1. A-simple t-test was carried out within each order of aberration with test variable zero. In figure 4.1, the Zernike coefficients without asterisks were not significantly different from zero; however, Zernike coefficients with one, two and three asterisks were significantly different from zero at 5%, 1% and 0.1% significance level, respectively. The third order coma and trefoil terms were significantly different from zero at 0.1% level of significance except $C^3_{3,}$ which was significant only at the 5% significance level. The spherical aberration term (C^0_4) was considerably larger than other forth order aberration terms; however, it was significant only at the 5% level of significance. The positive and negative values of coefficients cancel each other and hence the average value of Zernike coefficients seemed small. The absolute values of the Zernike coefficients represent the true aberration. Therefore, absolute values of Zernike coefficients along with standard deviations were plotted in Fig 4.2

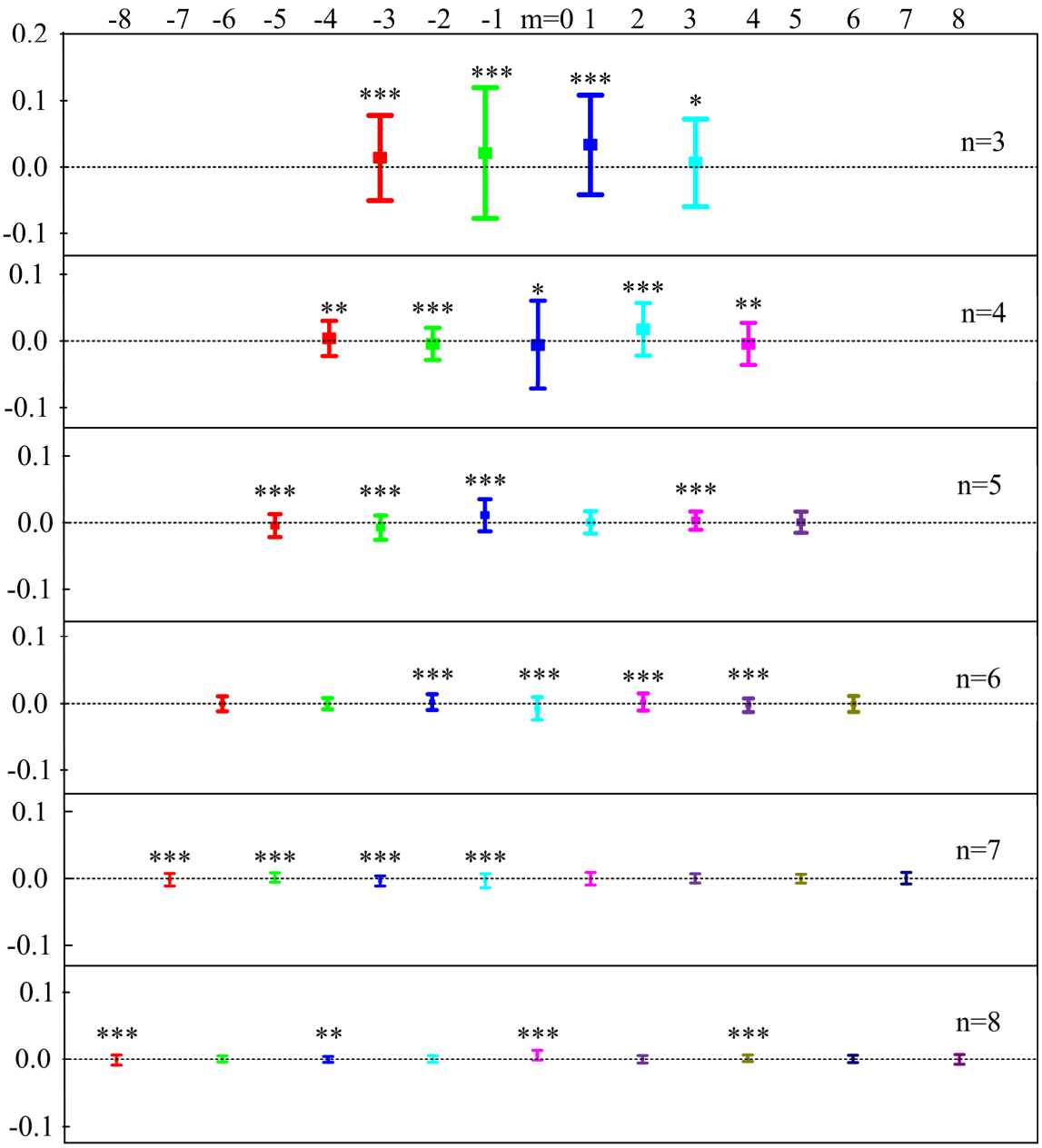

Figure 4:1 Zernike coefficient from 3rd to 8th order. A-simple t-test was carried out within each order of aberration with test variable zero. Zernike coefficients with one, two and three asterisks were significantly different from zero at 5%, 1% and 0.1% significant level, respectively, whereas Zernike coefficients without asterisks were not significantly different from zero.

Table 4:2 Mean values of higher order aberrations at different age

Aberrations	3 years	4 years	5 years	6 years	p-value
HOA	0.193±0.064	0.178±0.068	0.182±0.068	0.168±0.048	0.070
TC	0.124±0.062	0.116±0.067	0.119±0.065	0.102±0.046	0.254
TT	0.094±0.049	0.079±0.040	0.087±0.048	0.079±0.038	0.015
TSA	0.054±0.038	0.058±0.042	0.055±0.036	0.063±0.043	0.635
Third order	0.155±0.066	0.140±0.068	0.146±0.068	0.127±0.049	0.044
Fourth Order	0.085±0.038	0.083±0.040	0.077±0.039	0.083±0.040	0.662
Fifth Order	0.042±0.020	0.041±0.017	0.044±0.020	0.039±0.017	0.618
Sixth Order	0.032±0.013	0.030±0.012	0.031±0.014	0.029±0.011	0.394
Seventh Order	0.023±0.011	0.022±0.008	0.022±0.010	0.019±0.006	0.107
Eighth Order	0.019±0.008	0.019±0.007	0.019±0.009	0.014±0.004	0.004

Mean values of total HOA, TC, TT and TSA were shown in Table 4.2. The multivariate analysis of variance showed significance difference ($p=0.03$) in higher order aberrations between 3, 4, 5, and 6 years age groups. Mean RMS values of total HOA, total coma, total trefoil and total spherical aberration are plotted in Fig 4.3. Similarly, mean values of total third, fourth, fifth and the sixth order aberrations are plotted in Fig 4.4. The Bonferonni post-hoc test was carried out to test individual higher order aberrations; the significance level was fixed at $p<0.05/4$ to maintain the overall significance level of ($p<0.05$). When individual higher order aberrations were tested, total trefoil and total eighth order aberrations were significantly different among different age groups (Table 4.2). Mean RMS values of total

higher order aberrations were 0.193±0.064 μm, 0.178±0.068 μm, 0.182±0.068 μm and 0.168±0.048 μm for 3, 4, 5 and 6 year old children, respectively. These values slightly decreased with age. There was no significant difference (p=0.070) in the RMS values of total HOA between different age groups; however, p-values were close to the significance level. A significant negative correlation (r=-0.111, p=0.02) was observed between the total higher order aberrations and age (Fig 4.5). The highest aberration after total HOA was coma. The mean RMS values of the total coma for 3, 4, 5, and 6 year old age groups were 0.124±0.062 μm, 0.116±0.067 μm, 0.119±0.065 μm and 0.102±0.046 μm, respectively. The results showed that RMS values of coma slightly decrease with age; however, the mean values were not significantly different (p=0.254) among different age groups. The correlation coefficient was negative (r=-0.085, p=0.076) but no significant correlation was observed between the total coma and age; however, the p-value was close to the significance level (Fig 4.6). The mean RMS values of the total trefoil were 0.094±0.049 μm, 0.079±0.040 μm, 0.087±0.048 μm and 0.079±0.038 μm for 3, 4, 5, and 6 year old age groups, respectively. RMS values of trefoil declined with age and mean values were not significant (p=0.015). However, the Bonferonni post hoc test carried out to test multiple comparisons showed that there was a significant difference ($p<0.05/4$) in the total trefoil values between three year old and four year old children, whereas the rest of the inter-group comparisons were not significantly different ($p>0.05/4$). That was surprising because none of the inter-groups comparisons were expected to be significantly different. The Pearson correlation coefficient was negative (r=-0.103, p=0.031) and a significant association was observed between the total trefoil and age (Fig 4.7).

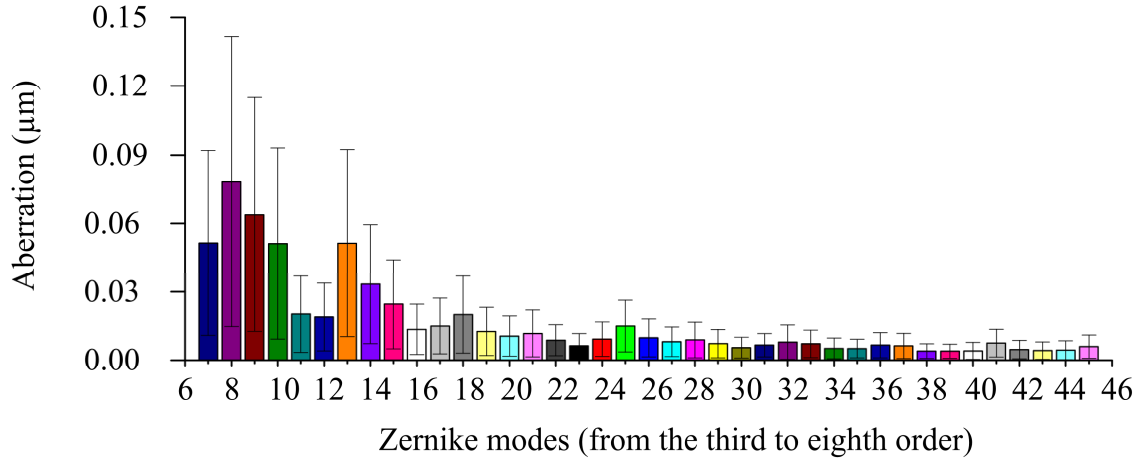

Figure 4:2 Average values of absolute Zernike coefficients from the 3rd to the 8th order.

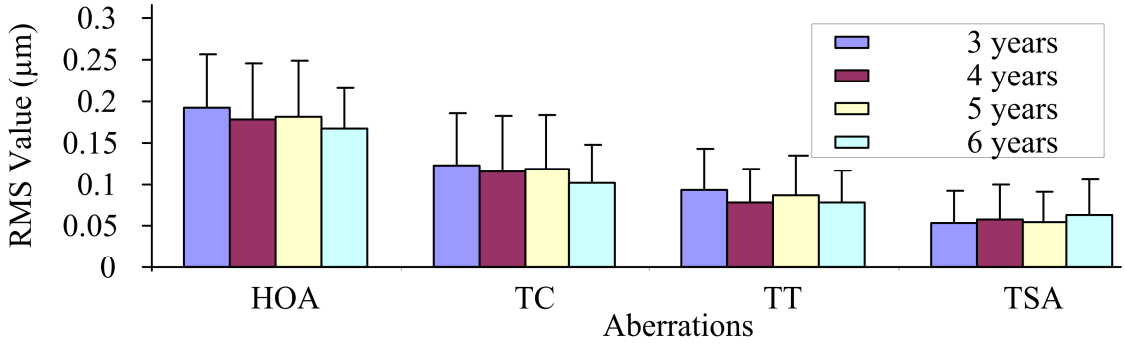

Figure 4:3 Comparisons of HOA, TC, TT and TSA among 3, 4, 5, and 6 year old children. Only trefoil was significantly different between 3 and 4 years children.

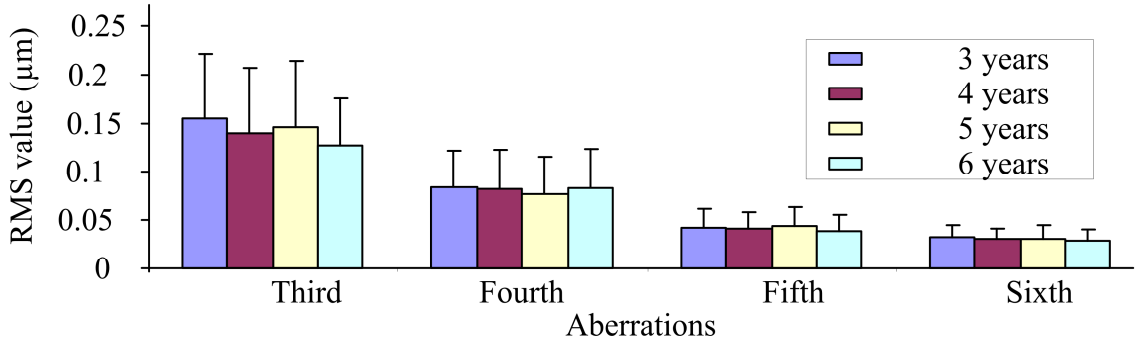

Figure 4:4 Comparisons of total third, fourth, fifth and sixth order aberrations among 3, 4, 5, and 6 year old children. None of them were significantly different among ages.

The most prominent higher order term in fourth order aberrations was the spherical aberration term, C^0_4. The mean RMS values of total spherical aberration were $0.054\pm0.038\,\mu m$, $0.058\pm0.042\,\mu m$, $0.055\pm0.036\,\mu m$ and $0.063\pm0.043\,\mu m$ for 3, 4, 5, and 6 year old children, respectively. Although the RMS values of spherical aberration increased with age, there was no significant difference (p=0.635). The spherical aberration was the only aberration term which increased with age in our sample. The correlation coefficient (r=0.047, p= 0.328) was positive but no significant correlation was observed between the total spherical aberration and age (Fig 4.8).

Table 4:3 Correlation analyses between higher order aberrations and age

Aberrations	Correlation (r)	p- value	Significantly correlated (p<0.05)
HOA	-0.111	0.02	Yes
TC	-0.085	0.076	No
TT	-0.103	0.031	Yes
TSA	0.047	0.328	No
Third order	-0.114	0.017	Yes
Fourth Order	-0.036	0.448	No
Fifth Order	-0.018	0.702	No
Sixth Order	-0.069	0.149	No
Seventh Order	-0.100	0.037	Yes
Eighth Order	-0.141	0.003	Yes

When between-groups effects (individual higher order aberrations) were observed, the third order aberrations were not significantly different (p=0.044) between different age groups. However, the p-value was very small and the mean RMS values declined with age.

The mean RMS values of the third order aberration were 0.155±0.066 μm, 0.140±0.068 μm, 0.146±0.068 μm, and 0.127±0.049 μm for 3, 4, 5, and 6 year old age groups, respectively (Fig 4.4). A significant negative correlation (r=-0.114, p=0.017) was observed between the third order aberration and age (Fig 4.9). Mean RMS values of the fourth order aberrations for different age groups (3, 4, 5 and 6 year olds) were 0.085±0.038 μm, 0.085±0.038 μm, 0.083±0.040 and 0.077±0.039 μm, respectively. Despite the fact that the mean RMS values declined with age, there was no significant difference (p=0.662). Furthermore, there was no significant correlation (r=-0.036, p=0.448) observed between the fourth order aberration and age (Fig 4.10).

Similarly, there was not a significant difference (p=0.618) between the RMS values of the fifth order aberrations 0.042±0.020 μm, 0.041±0.017 μm, 0.044±0.020 μm, 0.039±0.017 μm across 3, 4, 5 and 6 year old age children, respectively. The fifth order aberrations was not correlated to any significant degree (r=-0.018, p=0.702) with age. Mean RMS values of the sixth order aberrations 0.032±0.013 μm, 0.030±0.012 μm, 0.031±0.014 μm and 0.029±0.011 μm were not also significantly different (p=0.394) among 3, 4, 5, and 6 year old children, respectively. The sixth order aberration declined with age; however, there was no significant correlation (r=-0.069, p=0.149).

The RMS mean values of the seventh order aberrations were 0.023±0.011 μm, 0.022±0.008 μm, 0.022±0.010 μm and 0.019±0.006 μm for the respective age groups declined with age; however, there was no significant difference (p=0.107). A significant negative correlation (r=-0.100, p=0.037) was observed between the seventh order aberrations

and age. Similarly, the eighth order aberration was significantly correlated (r=-0.141, p=0.003) with age. The mean RMS values of the eighth order aberrations were $0.019\pm0.008\,\mu m$, $0.019\pm0.007\,\mu m$, $0.019\pm0.009\,\mu m$ and $0.014\pm0.004\,\mu m$ for 3, 4, 5, and 6 year old children, respectively. In-between group tests showed that the eighth order aberration was significantly different (p=0.004) among the age groups. When individual age groups were tested, the 6-year-olds were significantly different from the 3-year-olds (p=0.002) and 4-year-olds (p=0.004), where as other inter-age comparisons were not significantly different.

Major aberration coefficients ($C_3^{-3}, C_3^1, C_3^{-1}$, C_3^3 and $C^0{}_4$) were also compared among the four different age groups. The multivariate analysis of variance showed no significant difference (p>0.05) among different age groups (Fig 4.11). Although individual trefoil terms were not significantly different among the four different age groups, the total trefoil term was significantly different (p>0.05/4).

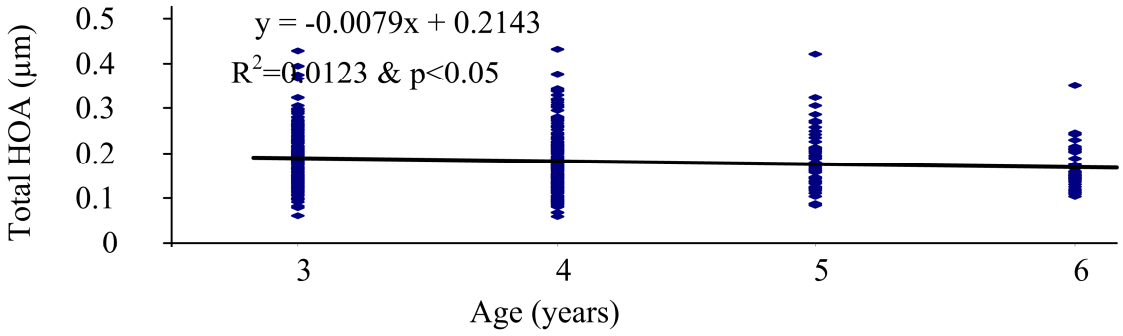

Figure 4:5 Correlations between total higher order aberrations and age. The correlation was significant (p<0.05).

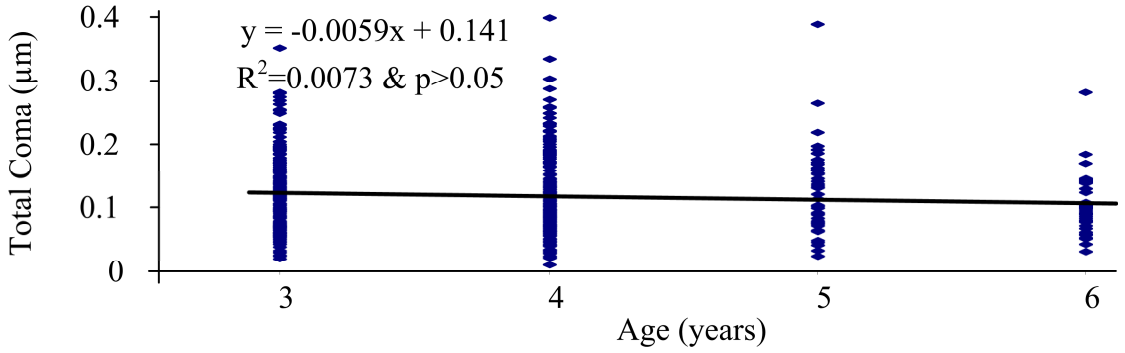

Figure 4:6 Correlation between total coma and age. No significant correlation was found between them ($p>0.05$).

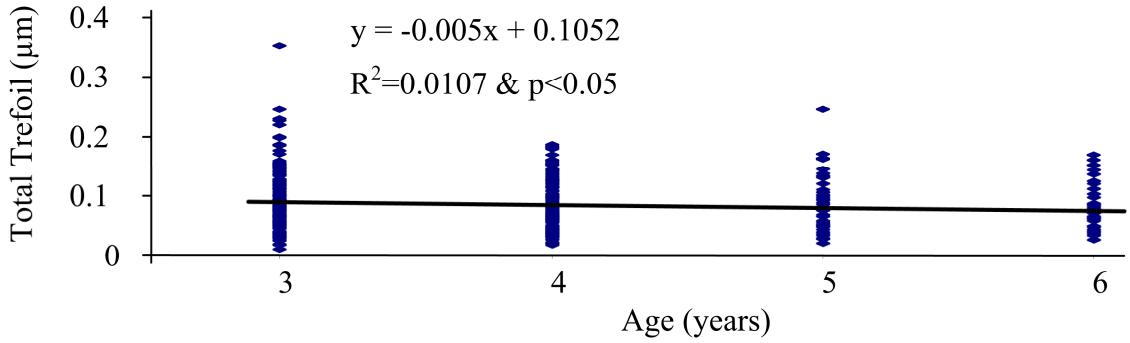

Figure 4:7 Correlation between total trefoil and age. Significant correlation was found between them ($p<0.05$).

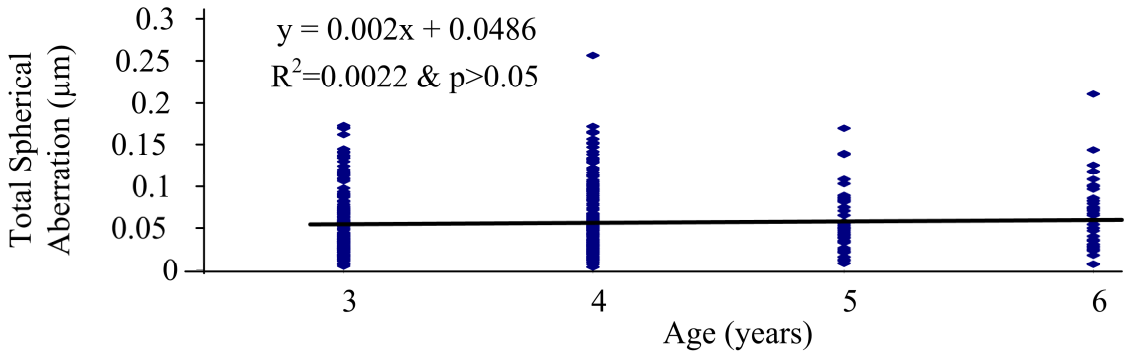

Figure 4:8 Correlation between total spherical aberration and age. No significant correlation was found between them ($p>0.05$).

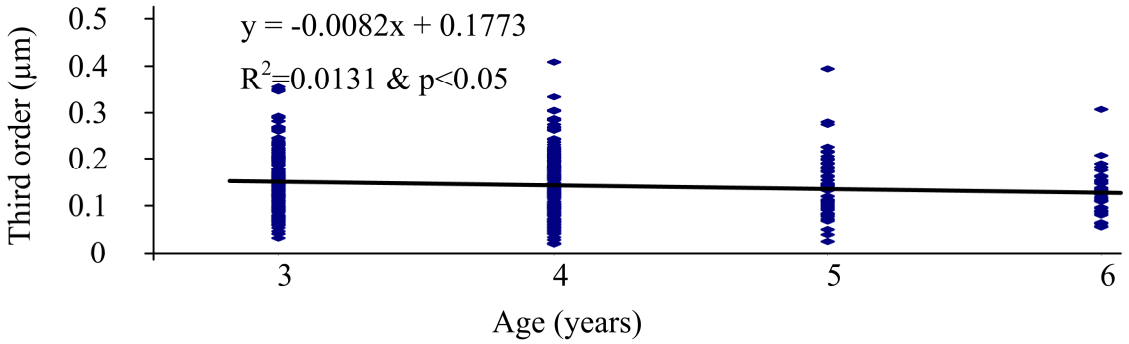

Figure 4:9 Correlation between total third order aberration and age. Significant correlation was found between them ($p<0.05$).

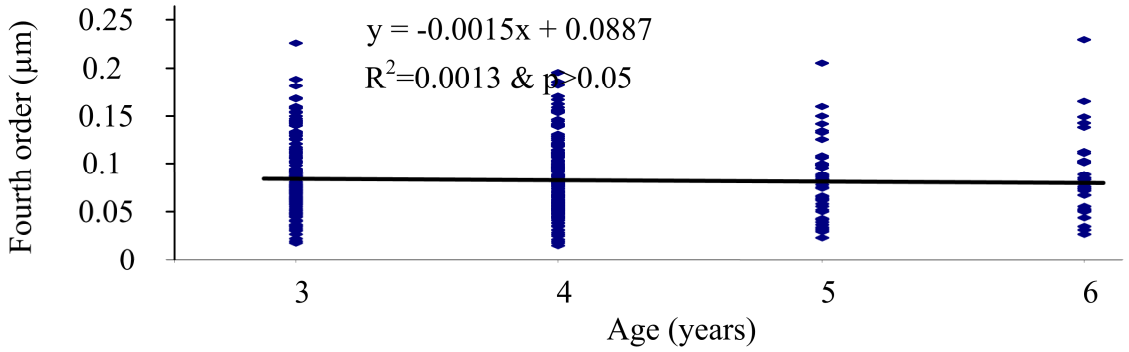

Figure 4:10 Correlation between total fourth order aberration and age. No significant correlation was found between them ($p>0.05$).

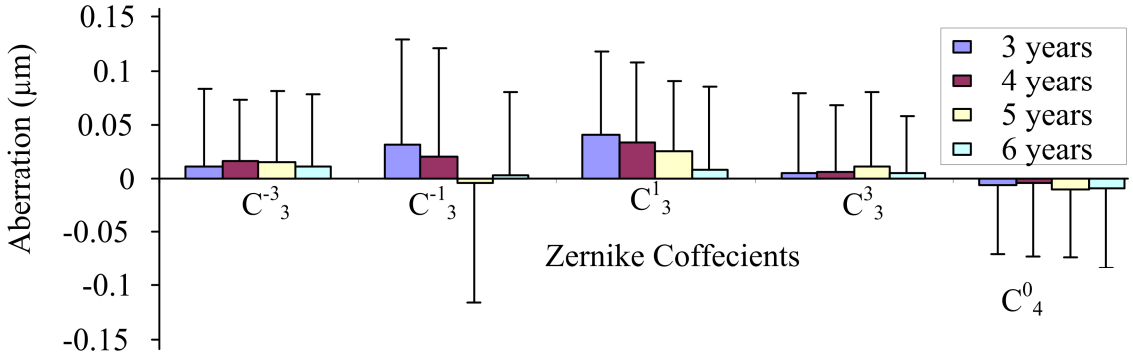

Figure 4:11 Comparison of $C_3^{-3}, C_3^1, C_3^{-1}$, C_3^3 and C^0_4 among 3,4,5 and 6 year old children. None of the coefficients were significantly different among different age groups.

4.4 Discussion

Brunette et.al[89] studied monochromatic aberration as a function of age from childhood to senior adults in a group of 114 subjects (mean age 43.2± 24.5 years, range 5 to 82 years). They calculated the Zernike coefficients from the 3rd to the 7th order for the pupil size of 5mm. They found that ocular aberration, in terms of the total RMS value, is at a maximum for children, it decreases gradually with time, becoming the lowest at the fourth decade of the life (37 years), and increases progressively with age. They concluded that higher order aberration decreases with the development of the optical structure of the eye. Although they used a broad range of ages, the number of subjects in each of the comparison groups was very small; there was a maximum of three subjects of the same age group.

Fujikado et al[84] studied age-related changes in ocular and corneal aberrations on the eyes of 66 normal subjects (aged 4–69 years; average 37.4 ±15.4 years). They found that coma-like aberrations, spherical-like aberrations and total aberrations of the whole eye were significantly correlated with age. However, the corneal aberrations alone were not correlated to any significant level. Because of the increase in lenticular higher order aberrations, the ocular aberration after 50-years-old was significantly increased in their sample. It should be noted that they had just 4 subjects less than 19 years old so the result can not be generalized. A very similar result was published by Kuroda et al[85]. They studied 76 visually normal subjects (range 4 to 69 years) and observed a weak correlation ($r=0.32$, $p=0.005$) between higher order aberrations and age.

He et al.[90] found significantly lower RMS values for total HOA in emmetropic children compared with myopic children. Carkeet et al[77] also observed slightly but significantly lower

spherical aberration in low myopia (-3.0 D<SE≤-0.5) compared with high myopia (SE≤-3.0D) (p=0.025) and emmetropes (-0.5<SE≤+1.0 D) (p=0.001). This supports our findings because hyperopia decreases with age from 3 to 6 years (Table 4.1). If refractive error correlates with higher order aberrations, then it might be correlated with the age of children; however, result could be different in the adult or older groups.

Artal et al.[81] compared the retinal image quality in terms of modulation transfer function between age groups in the late twenties and mid-sixties. The areas under the modulation transfer functions of younger subjects were always greater than that of the older subjects. A similar result was observed by Guirao et al.[66] in their subject sample, age ranges from 20 to 70 years. These studies showed that the retinal image quality of the eye progressively decreases with age from young adulthood to old age, which indicates that optical quality of the eye decrease with age. The optics of the eye gradually improves from birth to the time of emmetropization with the amount of aberration progressively decreased from 3 to 6 years in our study sample.

Salmon and Van de Pol[83] incorporated 10 other studies and observed the relationship between higher order aberrations and age of adult eyes (n=1,234). They found a significant correlation of RMS values for total higher order aberrations, total coma and total spherical aberration with age (r<0.20, p<0.01). They further showed significant correlations (p<0.01) of Zernike coefficients C_3^{-1}, C_3^1, and C_4^2 with age. For all the cases, the correlation coefficients were very small and data were collected across a broad range of ages so they concluded that factors other than age were also responsible for determining higher order aberrations of eyes.

The age related change of refractive error may have significantly affected the measured aberration levels. This chapter's study sample was large in a small age group, suggesting this study is more reliable for predicting the association between higher order aberrations and age; however, refractive error also decreases with age and this plays a greater role in determining the higher order aberrations of the individuals. All the cited studies had a wide range of refractive errors and the interaction of age on refractive error may have influenced their results. Relationship between aberration and age can be more accurately studied by taking subjects at different ages in a narrow range of refractive error. Atchison and Markwell[86] studied aberration of emmetropic subjects (spherical equivalent ranges from -0.88D to +0.75D) between 19 and 70 years age. They found a significant increase in on-axial aberration with age. Total higher order aberrations were increased by 26% across the age range in their sample. There were significant differences in the RMS value of the total higher order aberrations, the 4^{th} and the 5^{th} order aberrations. Horizontal coma was also significantly different between the ages. This study also showed a small change in higher order aberrations with respect to age. Greater age-related changes of ocular aberration may have been influenced by the greater variance in refractive error across subjects.

Jesson et al[87] studied higher order aberrations of the eye in young (20 to 30 year-olds) Indian university students. They observed no significant differences for total higher order aberrations among different age groups. The magnitude of aberration increased to some extent with age; however, there were no significant differences in aberration levels. This is exactly opposite to the result obtained by Brunnette et al[89]. The optics of the eye of a visually normal subject is almost the same from 20-40 years[18] so their study also supports that there is

small but gradual change in ocular aberration with age. Results of this chapter support that ocular aberration declines with age of the children and reaches a minimum at the time of emmetropization.

In summary, there are major anatomical and optical changes in the eyes of growing children. There was a question as to whether the major anatomical and optical changes in the eye stimulate different levels of monochromatic aberrations. The results of this chapter showed that ocular aberrations in terms of RMS values were at a maximum for 3 year old children, decreased gradually with age and the lowest aberrations were found for 6 year old children. This suggests that higher order aberrations also reduce during emmetropization. The exact relationship between emmetropization and the reduction of high order aberrations is not clear at this point.

Chapter 5

Strehl Ratio and Visual Acuity in a Pre-school Sample

5.1 Introduction

In spite of the popularity of wavefront guided surgery, the relationship between higher order aberrations and visual acuity is not clear; however, it has been stated that refractive laser eye surgeries like Radial keratomy (RK),[91] photorefractive keratectomy (PRK)[92,93] and laser insitu keratomileusis (LASIK)[92,94] induce higher order aberrations. Previous studies[95-98] suggest that visual performance of the eye could be improved by reducing higher order aberrations. Seiler et al[96,97] applied wavefront guided surgery and reported the possibility of obtaining the supernormal vision 6/3.6 (i.e. 20/12) or better. Binocular visual acuity of 6/12 or worse has been shown to improve by at least two Snellen lines after the correction of wavefront aberration by an unidentified refractive error called aberropia[99]. Aberropia refers to the improvement in vision or simply visual acuity by correcting waverfront aberration[99]. This finding suggested that higher-order aberrations negatively affect visual performance.

Other studies[100,101] have shown that there is very small effects of higher order aberrations on visual performance. Applegate et al[100] further suggested that this small deficit in visual performance is due to the normal variation in neural transfer functions across the subjects. Hong et al[101] studied the variation of visual performance and RMS values of wavefront error of visually normal optometry students and also observed a small effect on visual performance.

It has also been shown that the higher order aberrations of supernormal vision (VA 6/4.5 or better) are comparable to the higher order aberrations found in myopic eyes[78]. Kim et al[79] compared the higher order aberrations of supernormal vision (visual acuity 6/3.6) and high myopic groups (greater than -6D) and observed no significant difference in higher order aberrations. These results suggested that higher order aberrations may not be the perfect predictors of the visual performance.

The optical performance of the eyes in terms of the modulation transfer function (MTF) and Strehl ratio can be compared to examine the effect of aberration on the image quality of the eye. So the main purpose of this chapter's study is to compare the visual performance of the eye in terms of MTF and the Strehl ratio among the three different visual acuity groups (6/6, 6/9 and 6/12) in a large sample of pre-school children.

5.2 Methods

5.2.1 Subjects

All 834 images of 436 children (right eye 436 and left eye 399) were suitable for this study; however, this chapter is mainly focused on the comparison of Strehl ratios between three different visual acuity groups (i.e. 6/6, 6/9 and 6/12). A total of 781 eyes of 416 children (mean age 3.94± 0.94 years, range 3 to 6 years; right eye 404 and left eyes 377) met this criterion and hence they were included in this analysis. The sample showed a mean spherical equivalent of 1.19 ± 0.59D, a mean with-the-rule astigmatism of 0.055 ± 0.22D, and a mean oblique astigmatism of 0.011±0.14D. The visual acuity of the subjects varied

from 6/6 to 6/12. The visual acuity was measured using the single letter chart found in Cambridge Crowding Cards (Clement Clarke, Co, UK) described in Chapter 2. A complete description of the subjects divided by visual acuities is presented in Table 5.1. CCC testing was conducted in accordance to strict methodological procedures outlined by the manufacturer. All measures were taken with the child's refractive error corrected and the eyes cyclopleged.

Table 5:1 Demographic summary of the subjects

VA	n	Sp. Eq. (Mean ± SD)	J_0 (Mean ± SD)	J_{45} (Mean ± SD)
6/6	575	1.17±0.54D	0.046±0.18D	0.012±0.11D
6/9	180	1.28±0.65D	0.064±0.25D	0.005±0.17D
6/12	26	1.17±1.0D	0.20±0.45D	0.049±0.32D
Total	781	1.19 ± 0.59D	0.055 ± 0.22D	0.011±0.14D

5.2.2 Data analysis

Higher-order aberrations were presented as root mean square (RMS) values. In this chapter; (a) Zernike coefficients from 3rd to 8th orders; (b) root mean square (RMS) of higher order aberrations from 3rd to 8th orders; (c) Total coma (RMS of C_3^1, C_3^{-1}, C_5^{-1} C_5^1 and C_7^1, C_7^{-1}); (d) total trefoil (RMS of C_3^3, C_3^{-3}, C_5^3, C_5^{-3} and C_7^3, C_7^{-3}); and (e) total spherical aberration (RMS of C_4^0, C_6^0 and C_8^0 were computed. Higher order aberrations from the third to the eighth order were also compared among three different visual acuity groups.

Modulation transfer function (MFT) can be compared in three different visual acuity groups to examine the effect of aberration on the retinal image quality of the eye. The image of the point object formed by the optics of the eye is called a point spread function (PSF) which can be calculated by the Fourier transform of generalized exit pupil function. Fourier transform of PSF gives the optical transform function (OFT). The modulation transfer function is the real part of the OTF. In this study the area under the modulation transfer function of each subject was calculated and the average area under the MTF was compared among the different visual acuity groups.

The Strehl ratio also characterized the retinal image quality of the eye[102]. The ratio is generally defined as the ratio of the intensity peak of the real eye system and the intensity peak of the diffraction limited system. In this study we computed the simplified Strehl ratio, which is the ratio of the area under the MTF of the real eye and the area under the MTF of the diffraction limited eye.

The data were analyzed using SPSS (version 17.0). Multivariate analysis of variance was used to examine the effect of visual acuity on higher order aberrations. Hotelling's trace method was used to calculate the significance levels with a significance level fixed at 0.05. If multivariate analysis of variance showed a significant difference in higher order aberrations among different visual acuity groups, then the Bonferonni post-hoc test was carried out to test multiple comparisons.

5.3 Results

A total of 781 eyes were divided into three 6/6, 6/9 and 6/12 acuity groups and analyzed by their RMS values of aberrations, modulation transfer functions and Strehl ratios. Table 5.2 shows mean (± STD) values of higher order aberrations for three different visual acuity groups. The multivariate analysis of variance showed that higher order aberrations were significantly different (p=0.021) among visual acuity groups. The Bonferonni post-hoc test was carried out to test multiple comparisons and the significance level was fixed at p=0.05/3 to maintain the overall significant level of ($p<0.05$). When the between-groups test (i.e. individual higher order aberrations) was carried out, only total trefoil was significantly different ($p<0.05/3$) among different acuity groups. Mean values of total higher order aberrations, total coma, total trefoil and total spherical aberration were plotted in Fig 5.1. A similar multiple bar diagram was plotted for the mean values of total third, fourth, fifth and the sixth order aberrations in Fig 5.2.

Mean RMS values of total HOA from 3^{rd} to 8^{th} order were $0.1828\pm0.0640\,\mu m$, $0.1922\pm0.0755\,\mu m$, $0.2173\pm0.1141\,\mu m$ for visual acuity groups 6/6, 6/9 and 6/12, respectively. Mean RMS values of total HOA increased with decreased in visual acuity; however, the differences between the mean values were not significant (p=0.019). The mean RMS values of the total come were $0.1176\pm0.0649\,\mu m$, $0.1222\pm0.0732\,\mu m$ and $0.1329\pm0.0922\,\mu m$ for 6/6, 6/9 and 6/12 visual acuity groups, respectively. No significant differences (p=0.422) in mean RMS values of the total coma were observed. The mean RMS values of the total trefoil for 6/6, 6/9 and 6/12 visual acuity groups were $0.0848\pm0.0431\,\mu m$, $0.0923\pm0.0468\,\mu m$, $0.1197\pm0.0803\,\mu m$, respectively. Significant difference ($p<0.01$) in the

total trefoil among different visual acuity groups was observed. When individual visual acuity groups were tested, the Bonferonni post-hoc test showed that the total trefoil of the 6/6 visual acuity group was significantly lower ($p<0.01$) than that of the 6/12 visual acuity group. The rest of the inter-acuity comparisons were not significantly different ($p>0.05/3$) for the total trefoil. Mean RMS values of the total spherical aberration were $0.0561 \pm 0.0391\,\mu m$, $0.0552 \pm 0.0394\,\mu m$ and $0.0624 \pm 0.0366\,\mu m$ for 6/6, 6/9 and 6/12 visual acuity groups. No significant differences in mean values were observed ($p=0.687$).

Table 5:2 Mean values of higher order aberrations between different levels of visual acuity

Aberrations	6/6	6/9	6/12	p-value
HOA	0.1828 ±0.0640	0.1922 ±0.0755	0.2173 ±0.1141	0.019
TC	0.1176 ±0.064	0.1222 ±0.0732	0.1329 ±0.0922	0.422
TT	0.0848 ±0.0431	0.0923 ±0.0468	0.1197 ±0.0803	0.000
TSA	0.0561 ±0.0391	0.0552 ±0.0394	0.0624 ±0.0366	0.687
Third	0.1447 ±0.0652	0.1536 ±0.0739	0.1758 ±0.1151	0.038
Fourth	0.0820 ±0.0381	0.0871 ±0.0405	0.0959 ±0.0349	0.077
Fifth	0.0424 ±0.0174	0.0434 ±0.0195	0.0466 ±0.0243	0.436
Sixth	0.0300 ±0.0123	0.0305 ±0.0125	0.0351 ±0.0171	0.136
Seventh	0.0223 ±0.0096	0.0224 ±0.0097	0.0270 ±0.0138	0.055
Eighth	0.0185 ±0.0076	0.0185 ±0.0076	0.0213 ±0.0087	0.186

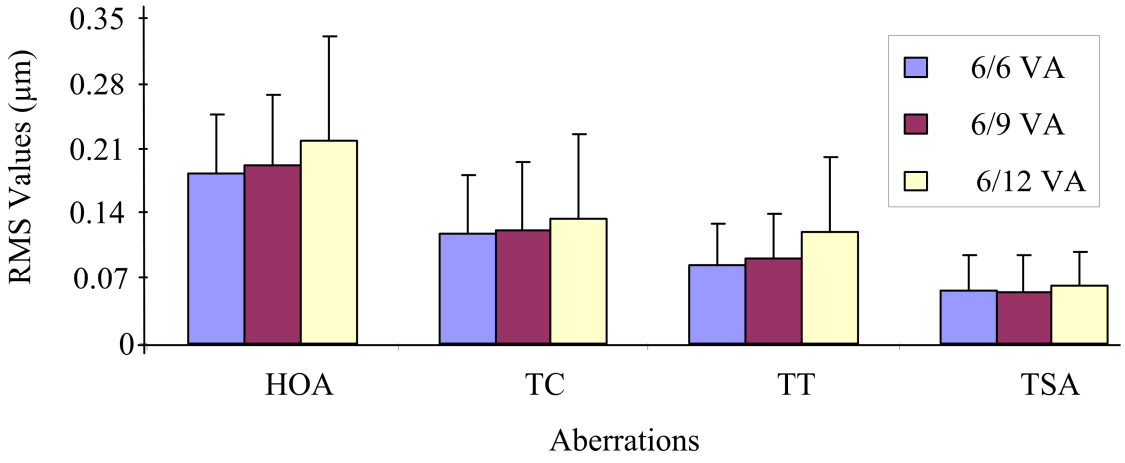

Figure 5:1 Mean values of total higher order aberration, total coma, total trefoil and total spherical aberration. Significant difference in total trefoil between 6/6 and the 6/12 groups was found whereas rest of the comparisons were not significant.

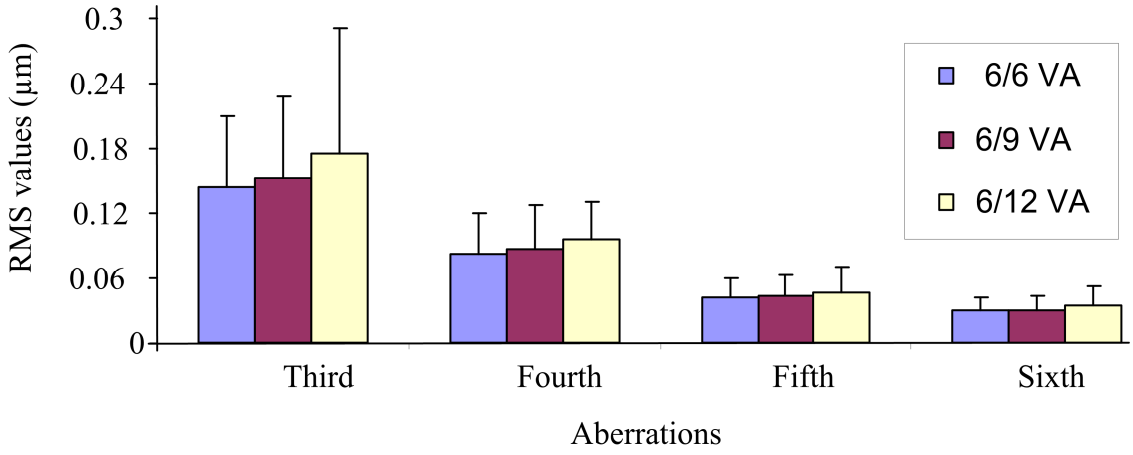

Figure 5:2 Mean values of total third, fourth, fifth and sixth order aberrations. No significant differences in higher order aberrations across visual acuities groups were found ($p<0.05/3$).

In this study, slightly lower levels of aberrations was found for 6/6 acuity group than the 6/12 acuity group. Some of the higher order aberrations were significantly different among the visual acuity groups while some were not. The third order aberration was the largest among the higher order aberrations. The mean RMS values of the third order aberration were

0.1447 ±0.0652 μm, 0.1536 ±0.0739 μm and 0.1758 ±0.1151 μm for 6/6, 6/9 and 6/12 visual acuity groups, respectively. No significant differences (p=0.038) in mean RMS values of the third order aberration were found. The mean RMS values of the fourth order aberration were comparable among different visual acuity groups. The mean values were 0.0820 ±0.0381 μm, 0.0871 ±0.0405 μm and 0.0959 ±0.0349 μm for 6/6, 6/9 and 6/12 visual acuity groups, respectively. No significant difference (p=0.077) in the fourth order aberration was found for different acuity groups.

The mean RMS values of the fifth order aberration for 6/6, 6/9 and 6/12 acuity groups were 0.0424 ±0.0174 μm, 0.0434 ±0.0195 μm and 0.0466 ±0.0243 μm, respectively. They were not significantly different (p=0.436). The mean RMS values of the sixth order aberration were 0.0300 ±0.0123 μm, 0.0305 ±0.0125 μm and 0.0351 ±0.0171 μm for 6/6, 6/9 and 6/12 acuity groups, respectively and no significant difference (p=0.136) was observed among the mean values. The RMS mean values of the seventh order aberration were 0.0223 ±0.0096 μm, 0.0224 ±0.0097 μm and 0.0270 ±0.0138 μm for 6/6, 6/9 and 6/12 acuity groups, respectively. No significant difference (p=0.055) in the seventh order aberration among different acuity groups was found. Similarly, the mean RMS values of the eighth order aberration were 0.0185 ±0.0076 μm, 0.0185 ±0.0076 μm and 0.0213 ±0.0087 μm for 6/6, 6/9 and 6/12 acuity groups, respectively. No significant difference (p=0.186) in the mean values of the eighth order aberrations were found.

Modulation Transfer Functions of 6/6, 6/9 and 6/12 visual acuity groups were plotted in Fig 5.3, 5.4 and 5.5, respectively. The red color MTF was the average MTF of that particular acuity group. The mean MTFs of different acuity groups were compared in Fig 5.6. The area under the MTF varied across individuals with the standard deviation of 5.99 a. u. The mean (± STD) area under the MTF for the 6/6 visual acuity group was 21.57±5.4 a. u., for 6/9 was 21.14± 5.8a.u, and for 6/12 was 20.3± 6.0 a. u. One-way ANOVA was carried out to examine the differences in areas across the three different visual acuity groups. The mean areas were not significantly different (p=0.381).

Strehl ratios were calculated from the MTF. The average (± STD) Strehl ratio of the 6/6 visual acuity group was 0.516± 0.13, for 6/9 it was 0.506±0.14, and for 6/12 it was 0.485±0.14. The average Strehl ratios among the different visual acuity groups were not statistically significant (p=0.381) Fig 5.7.

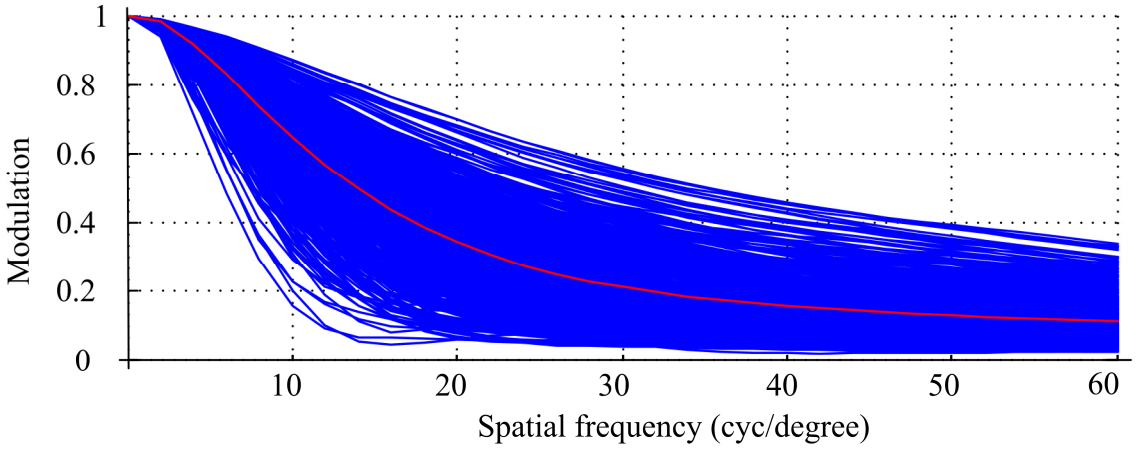

Figure 5:3 Modulation transfer function of all subjects of the 6/6 visual acuity group. The area under the MTF varied from individual to individual within this group with the standard deviation of 5.4 a. u.

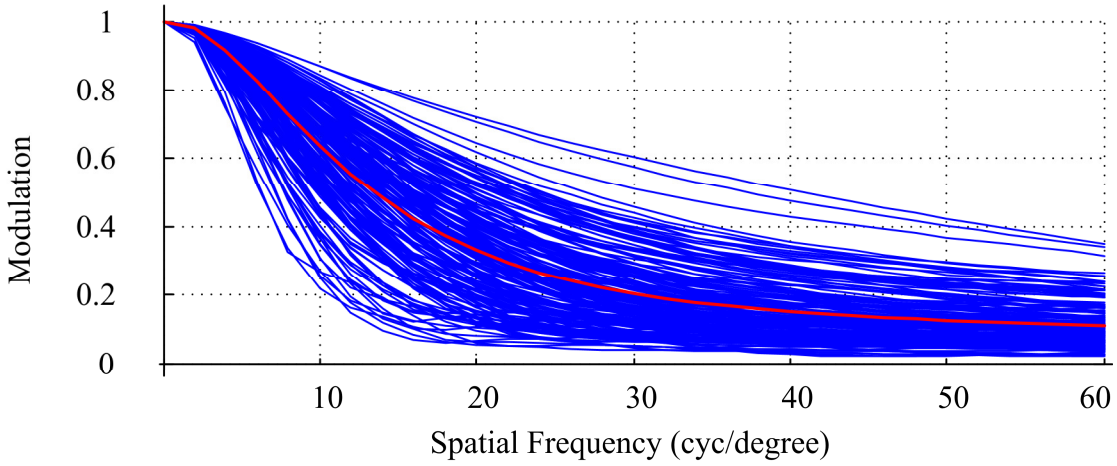

Figure 5:4 Modulation transfer function of all subjects of the 6/9 visual acuity group. The area under the MTF varied from individual to individual within this group with the standard deviation of 5.8 a. u.

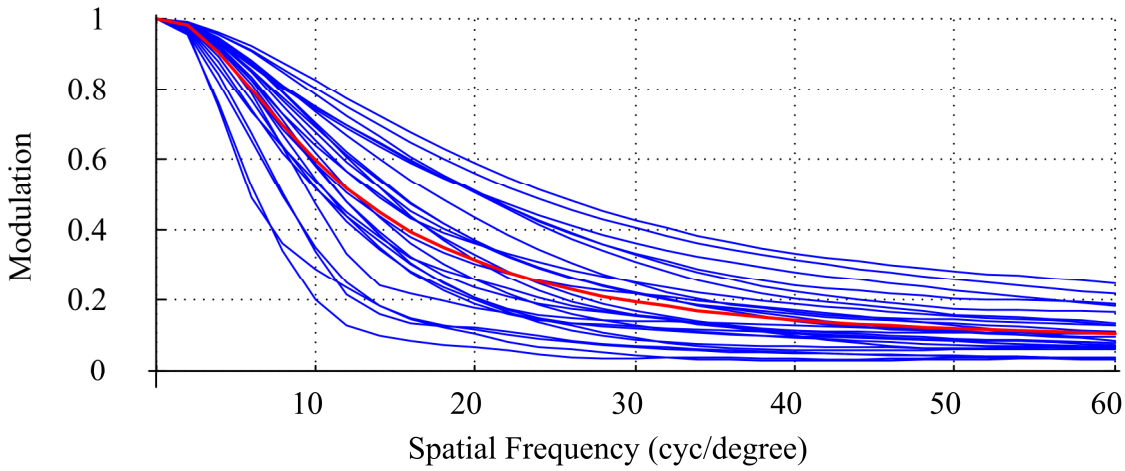

Figure 5:5 Modulation transfer function of all subjects of the 6/12 visual acuity group. The area under the MTF varied from individual to individual within this group with the standard deviation of 6.0 a. u.

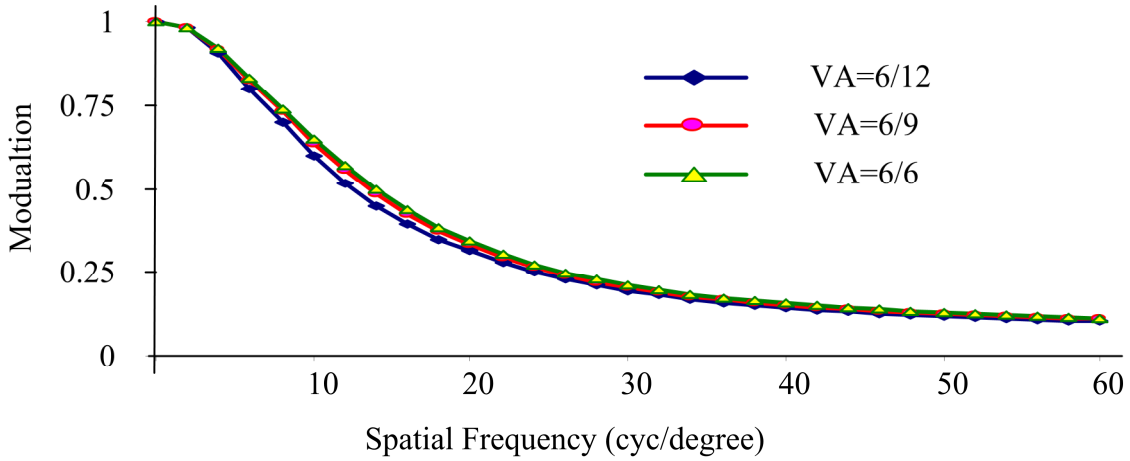

Figure 5:6 Mean modulation transfer function of 6/6, 6/9 and 6/12 visual acuity groups. Area under the modulation transfer function of all the subjects were calculated and compared. No significant difference (p=0.381) in the area under the MTF across the three different visual acuity group was found.

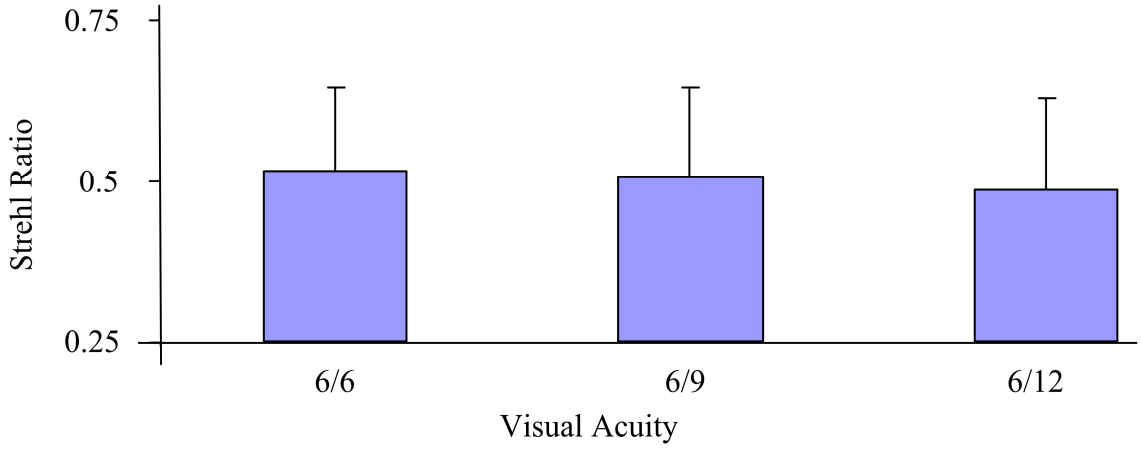

Figure 5:7 Mean Strehl ratios of 6/6, 6/9 and 6/12 visual acuity groups. No significant difference in Strehl ratios was found.

5.4 Discussion

In this study, higher order aberrations of hyperopic pre-school children across a narrow range of age (3 to 6 years) were calculated. Visual acuity develops considerably from birth to the age of 1 year and after that it gradually increases; and around 5 years, the child usually has 6/6 level of visual acuity[7]. Therefore, at the age of three years the visual acuity is still developing so our sample shows the variation of acuity from 6/6 to 6/18. Visual acuity might be affected by abnormal amounts of refractive error in pre-school sample. Our sample included a small range of refractive errors and a small range of visual acuity; hence the ocular aberrations were comparable across the different acuity groups.

The results obtained in this chapter are slightly different from previous findings[78, 79]. Although, RMS values of aberration were lower for better acuity groups, they were not significantly different amongst the different groups, except for total trefoil. A significant difference ($p<0.05/3$) in the total trefoil was found between the 6/6 and the 6/12 visual acuity groups. This result is not surprising since in Chapter 6 of this thesis, a significant correlation ($p<0.05$) between the refractive error and higher order aberrations is shown. It is important to note that high hyperopes show reduced visual acuity even when corrected.[103,104] This result was also validated by Chapter 4 results as higher order aberrations were weekly correlated to the age of the children from 3 to 6 year. Multivariate analysis of variance between different age group (3, 4, 5 and 6 years) showed that there was a significant difference ($p=0.03$) in higher order aberrations among different age groups. Visual acuity develops from 3 to 6 years so if age weakly correlate with HOA, visual acuity might also be weekly correlated in the growing eyes of pre-school sample.

Some previous studies[95-98] showed that reducing the higher order aberrations can improve the visual performance of the eye. However, more recent studies showed no relation between visual acuity and higher order aberrations.[78,79] Levy et al.[78] studied 70 eyes of 35 adults (mean age 24.3±7.7) with supernormal vision (VA>6/4.5) using the Nidek OPD scan wavefront aberrometer, they found a considerable amount of higher order aberrations for the supernormal vision, which were comparable with that of myopic eyes observed by Wang et al[105]. A similar study was conducted by Kim el al[79] on a group of Koreans. They compared 54 eyes of 36 myopic subjects with greater than -6D of refractive error and 32 eyes of 20 subjects with uncorrected visual acuity of 20/12 and found no significant difference in higher order aberration between these groups.

Modulation transfer functions as well as Strehl ratio express the optical performance of the eye. They are not affected by the neural level and internal noise. We did not observe significant differences in MTFs and Strehl ratios among different visual acuity groups because optical parameters are not fully responsible for the visual performance of the eye[100]. Applegate et al[100] studied the variation of higher order aberrations with visual performance and found a low correlation between them for low levels of aberrations. They suggested that this small deficit in visual performance might be due to the variation in neural transfer function across the subjects. Finally, they concluded that for low levels of aberration, RMS values of wavefront aberrations are not perfect predictors of visual performance and they suggested the need to develop new metrics that correlate better with visual performance. Thibos et al[106] developed some metrics to predict visual acuity because of the limitations of

using RMS values as a perfect predictor of visual performance. More recently, Faylinejad[107] in our laboratory has implemented a computational model for predicting visual acuity from wavefront aberration measurements. She used a constant amount of neural transfer function calculated from the contrast sensitivity function and the optical transfer function. The noise level was varied from 20% to 120% of the signal. The most important finding she observed was that the noise level varies among individuals and that plays a significant role in visual acuity. This finding also suggests that MTF alone is not capable of perfectly describing the visual performance of the eye. Other metrics such as the neural transfer function, as well as the amount of neural noise are necessary to describe the resultant visual performance.

In summary, this study showed no significant difference in higher order aberrations among different (6/6, 6/9 and 6/12) visual acuity groups, except for total trefoil. This finding was strongly supported by Chapter 6 and Chapter 4 findings which have reveled significant correlations between the refractive error and higher order aberrations, and very week correlation between age and higher order aberrations, respectively. Theoretically, the lower the aberrations the better vision would be; this findings support this idea. This finding suggests that reduction of higher order aberrations might be fruitful for the improvement of refractive surgery; however, aberrations alone are not capable of perfectly describing the visual performance of the eye. Other matrices such as neural transfer function and neural noise are also responsible for the quality of vision. Wavefront-guided refractive surgery is becoming popular as patient satisfaction is greater than with other refractive surgeries such as RK, PRK and LASIK. Wavefront-guided refractive surgery corrects the refractive status of the patients beyond the lower order aberrations and theoretically patients achieve

supernormal vision. The relationship between higher order aberrations and visual acuity is important from a clinical point of view and considering this relationship may help to further develop wavefront-guided refractive surgery.

Chapter 6
Refractive Error and Higher Order Aberrations

6.1 Introduction

With growth, there is a correlation between the optical components and refractive power[7]. Refractive power has a high correlation with axial length of the eye[6]. Refractive error occurs if the refractive power and the axial length of the eye unevenly develop[7]. There is a question as to whether the development of the refractive error of the eye is associated with different levels of monochromatic higher order aberrations. Several studies have assessed the association of second order aberrations with higher order aberrations[76,77,108-114]. Significantly larger higher order wavefront aberrations have been reported in myopic eyes compared with emmetropic eyes in several studies of adults[90,108,109,110] and it has been hypothesized that higher order aberrations induce myopia. For example, He et al.[90] measured the monochromatic wavefront aberrations of emmetropic and moderately myopic school children and young adults. They found significant differences ($p<0.01$) in higher order aberrations between the emmetropes and myopes. Paquin et al[108], also observed the higher level of RMS values for aberrations with higher degrees of myopia; however, they observed a quasi-linear relationship between higher order aberrations and myopia. Others studies[76,77,111,112] have shown that there is no relationship between higher order aberrations and refractive error, suggesting that higher order aberration may not be a suitable predictor of refractive error. For example, Carkeet et al[77] reported monochromatic aberrations of 273 Singaporean school children and found no significant difference across refractive error groups. Wei et al[111] performed correlation analysis on a sample of Chinese adults with myopia and observed no

correlation (r= -0.011, p=0.886) between higher order aberrations and refractive error. Later studies[78, 79] showed that even the subjects with supernormal vision (visual acuity 20/15 or better) had significant amounts of higher order aberrations and no significant difference in higher order aberrations between supernormal vision and myopia. Other studies also show some controversial findings on the amount of higher order aberrations present in hyperopes and myopes. Kirwan et al[113] studied aberrations in children and found significantly greater levels of higher order aberrations in myopes compared with hyperopes; on the other hand, Lorente et al[114] observed a significantly larger (p=0.02) RMS values of third order aberrations for hyperopes compared with myopes. To date, no published study has described the variation of higher order aberrations from hyperopia to emmetropization of growing eyes. So the main purpose of this chapter was to study the variation of higher order aberrations in a group of pre-school children, in the age range of 3 to 6 years, in whom hyperopia gradually reduces with age.

6.2 Methods

6.2.1 Subjects

All 834 images of 436 children (right eye 436 and left eye 399) were suitable for this chapter's study; however, significant correlations in higher order aberrations between the eyes occur (see Chapter 3). So, only right eyes of the children were used herein. Furthermore, myopes were not included since they were very small in number (n=5) compared with emmetropes (n=42) and hyperopes (389). A total of four hundred and thirty one eyes were selected to examine the association between the refractive error and higher order aberrations

on the visually normal children (mean age 3.89± 0.92 years, range 3 to 6 years). The sample showed a mean spherical equivalent of 1.19±0.63D, a mean with-the-rule astigmatism of 0.058±0.22D, and a mean oblique astigmatism of 0.033±0.13D. Subjects were arbitrarily classified as, emmetropic (range -0.5 to +0.5D), low hyperopic (+0.5 to +2D) and high hyperopic (+2D or more) based on spherical equivalent. The visual acuity of the subjects varied from 6/6 to 6/18. The complete demographic descriptions of subjects divided in terms of spherical equivalent are shown in Table 6.1.

Table 6:1 Demographic descriptions of subjects divided in terms of spherical equivalent

Refractive error Groups	n	Sp. Eq. (Mean ± SD)	J_0 (Mean ± SD)	J_{45} (Mean ± SD)
Emmetropic	42	0.16±0.28D	0.014±0.18D	0.054±0.10D
Low hyperopic	356	1.22±0.36D	0.06±0.21D	0.030±0.12D
High hyperopic	33	2.44±0.31D	0.090±0.32D	0.049±0.24D
Total	431	1.19±0.63D	0.058±0.22D	0.033±0.13D

6.2.2 Data analysis

Higher-order aberrations are presented as root-mean-square (RMS) values. In this chapter; (a) RMS values of higher order aberrations from 3rd to 8th orders; (b) Total coma (RMS of C_3^1, C_3^{-1}, C_5^{-1} C_5^1 and C_7^1, C_7^{-1}); (c) total trefoil (RMS of C_3^3, C_3^{-3}, C_5^3, C_5^{-3} and C_7^3, C_7^{-3}); and (d) total spherical aberration (RMS of C_4^0, C_6^0 and C_8^0) were compared across refractive error groups. Variations of individual higher order aberrations from the 3rd to the 8th order across refractive error groups were also studied. Data analysis was done using statistical

software (SPSS version 17.0). Multivariate analysis of variance was used to examine the effect of refractive error on higher order aberrations. Hotelling's trace method was used to calculate the significance level to maintain a fixed significance level at 0.05. If multivariate analysis of variance showed a significant difference in higher order aberrations among different refractive error groups then the Bonferonni post hoc test was carried out to test multiple comparisons. Finally, Pearson correlation coefficients were calculated to examine the correlation between the higher order aberrations and refractive error.

6.3 Results

Association between the refractive errors and higher order aberrations of 431 right eyes were studied. Refractive errors were significantly different ($p<0.05$) among emmetropic, low hyperopic and high hyperopic groups (One-way ANOVA). The Bonferonni post hoc test carried out to assess multiple comparisons showed that, all the inter-refractive error groups were significantly different ($p<0.05/3$). One-way ANOVA conducted to examine the differences in with-the-rule astigmatism (J_0) among different refractive error groups showed no significant difference ($p=0.481$). No significant correlation was found between refractive error and with-the-rule astigmatism ($r=0.066$, $p=0.172$). Similarly oblique astigmatism (J_{45}) was not significantly different between different refractive error groups ($p=0.564$). Oblique astigmatism and refractive error were not correlated to any significant level ($r=-0.032$, $p=0.51$).

Table 6.2 shows the mean values of higher order aberrations with respect to different refractive error groups. The multivariate analysis of variance showed significant differences

in the pattern of higher order aberrations found between emmetropic, low hyperopic and high hyperopic refractive errors (Hotelling's trace method, $p<0.001$). When between-groups effects (individual higher order aberration) were observed, all the higher order aberrations (i.e. total HOA, total coma, total trefoil, total spherical aberration, total third, fourth, fifth, sixth, seventh and the eighth order) were significantly different ($p<0.05/3$) among different refractive error groups. So Bonferonni post hoc test was carried out to assess individual higher order aberrations and the significance level was fixed at $p=0.05/3$ to maintain the overall significant level of ($p<0.05$).

The Bonferroni post-hoc test carried out to test multiple comparisons within HOA showed that, total HOA of high hyperopic refractive error group was significantly greater than the emmetropic group ($p<0.01$) and the low hyperopic refractive error group ($p<0.01$). The emmetropic group was not significantly different from the low hyperopic group ($p>0.05/3$). Similarly the Bonferroni post hoc test of the total coma showed that the low hyperopic group was significantly different from the high hyperopic group ($p<0.01$) whereas the rest of the within-group comparisons were not significant ($p>0.05/3$). Total trefoil was significantly different among all the within-group comparisons ($p<0.01$). The total trefoil was significantly lower in the emmetropic group compare with both the low hyperopic group and the high hyperopic group. The Bonferroni post hot test of total spherical aberration showed that emmetropic group had a significantly ($p=0.014$) lower amount of TSA compared with the high hyperopic group, whereas all the other within-group comparisons were not significantly different in TSA. Fig 6.1 showed the comparison of mean RMS values of HOA, TC, TT and TSA across refractive error groups.

Table 6:2 Mean values of higher order aberrations among different refractive error groups

Aberrations	Emmetropic	Low hyperopic	High hyperopic	p-value
HOA	0.1620±0.0678	0.1816±0.0612	0.2429±0.0743	0.001
TC	0.1186±0.0729	0.1148±0.0613	0.1573±0.0681	0.001
TT	0.0617±0.0256	0.0864±0.0440	0.1128±0.0565	0.001
TSA	0.0470±0.0329	0.0561±0.0390	0.0731±0.0514	0.016
Third	0.1318±0.0717	0.1435±0.0631	0.1904±0.0748	0.001
Fourth	0.0662±0.0320	0.0822±0.0375	0.1132±0.0467	0.001
Fifth	0.0358±0.0128	0.0410±0.0173	0.0578±0.0269	0.001
Sixth	0.0257±0.0123	0.0308±0.0115	0.0387±0.0161	0.001
seventh	0.0186±0.0081	0.0221±0.0085	0.0299±0.0149	0.001
Eighth	0.0158±0.0071	0.0185±0.0070	0.0262±0.0126	0.001

Higher order aberrations from third to eighth order were also analyzed. The Bonferonnia post-hoc test with-in third, fourth, fifth, sixth, seventh and the eighth order aberrations showed that the high hyperopic group was significantly different from both the emmetropic ($p<0.01$) and the low hyperopic group ($p<0.01$), while no significant differences ($p>0.05/3$) was observed between the emmetropic and the low hyperopic group. Figure 6.2 showed the comparison of mean RMS values of total third, total fourth, total fifth, and the total sixth order aberrations across refractive error groups.

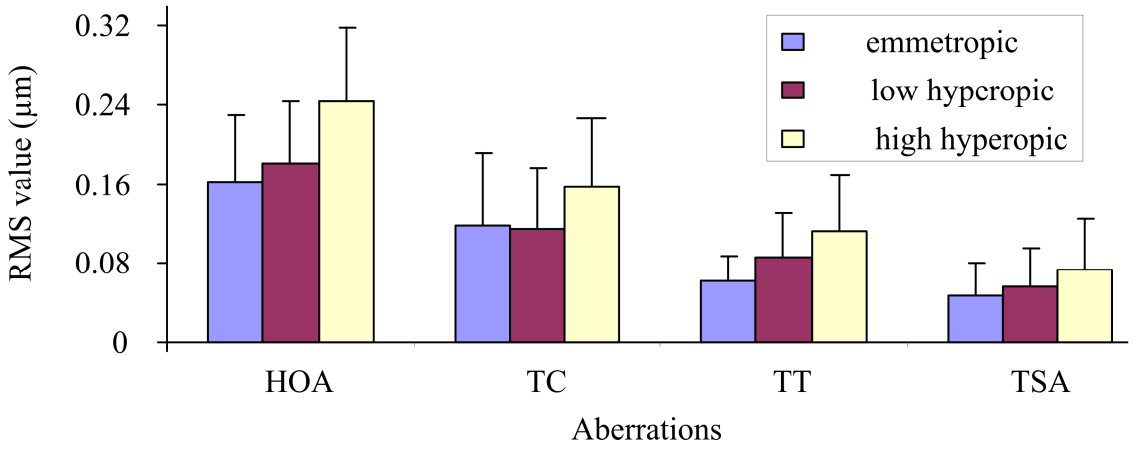

Figure 6:1 Comparison of RMS value of total higher order aberrations (HOA), total coma (TC), total trefoil (TT) and total spherical aberration (TSA) among emmetropic, low hyperopic and high hyperopic subjects. The mean values were significantly different ($p<0.02$) among refractive error groups.

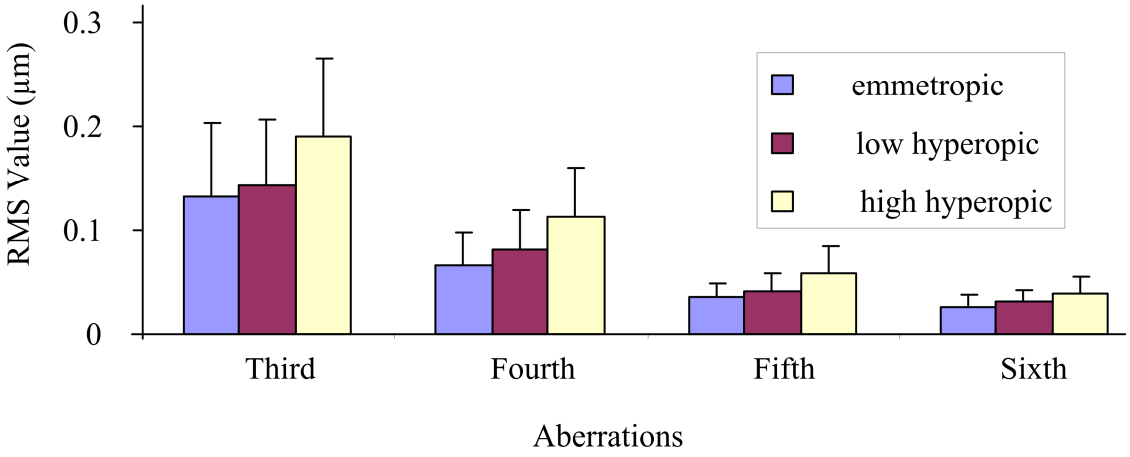

Figure 6:2 Comparison of RMS values of total third, fourth, fifth and sixth order aberrations among emmetropic, low hyperopic and high hyperopic subjects. The mean values were significantly different ($p<0.02$) among different refractive error groups.

Correlation analysis was conducted to examine the association of higher order aberrations with refractive error. The Pearson correlation coefficients (r) showed that all the higher order aberrations were significantly correlated ($p<0.01$) with refractive error. The correlation coefficients along with associated p-value are shown in Table 6.3. Liner fit was plotted for the total higher order aberrations and refractive errors (Fig 6.3). The fit showed that the aberration was small for emmetropic subjects and gradually increased with refractive errors.

Table 6:3 Correlation analyses between higher order aberrations and refractive error

Aberrations	Correlation (r)	p- value
HOA	0.245	0.001
TC	0.111	0.021
TT	0.237	0.001
TSA	0.133	0.006
Third order	0.174	0.001
Fourth Order	0.243	0.001
Fifth Order	0.236	0.001
Sixth Order	0.216	0.001
Seventh Order	0.244	0.001
Eighth Order	0.261	0.001

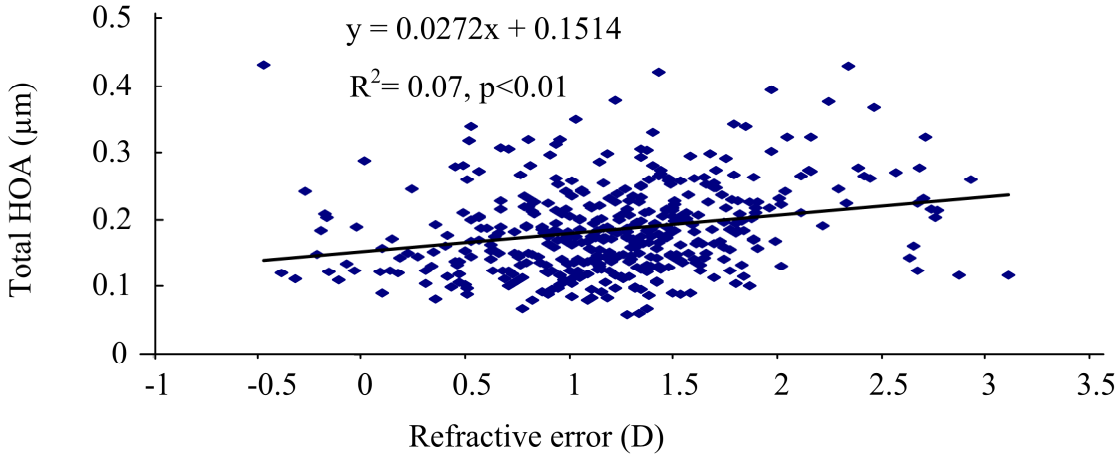

Figure 6:3 Linear fit between RMS values of total higher order aberrations from the third to the eighth order aberrations and refractive errors. Significant correlation ($p<0.01$) was found between the total HOA and refractive error.

Generalized Strehl ratios were calculated from the modulation transfer functions. The mean Strehl ratios of emmetropic, low hyperopic and high hyperopic subjects were 0.57±0.13 a.u., 0.52±0.13 a.u and 0.41±0.11 a.u, respectively. One-way ANOVA showed a significant difference ($p<0.01$) in the mean values of Strehl ratios across refractive error groups (Fig 6.4). When within-group comparisons were carried out the high hyperopic group had a significantly lower amount of Strehl ratios compared with the low hyperopic ($p<0.01$) and the emmetropic ($p<0.01$) groups. Although the Strehl ratio of emmetropic group was greater than that of the low hyperopic group, they were not significantly different ($p>0.05/3$). The correlation coefficient between Strehl ratio and refractive error was small ($r=-0.25$); however, a significant correlation was observed between them ($p<0.01$). Liner fit plotted between the Strehl ratios and refractive errors is shown in Figure 6.5. Strehl ratios were

largest for the emmetropic subjects and gradually decreased with increased in refractive errors.

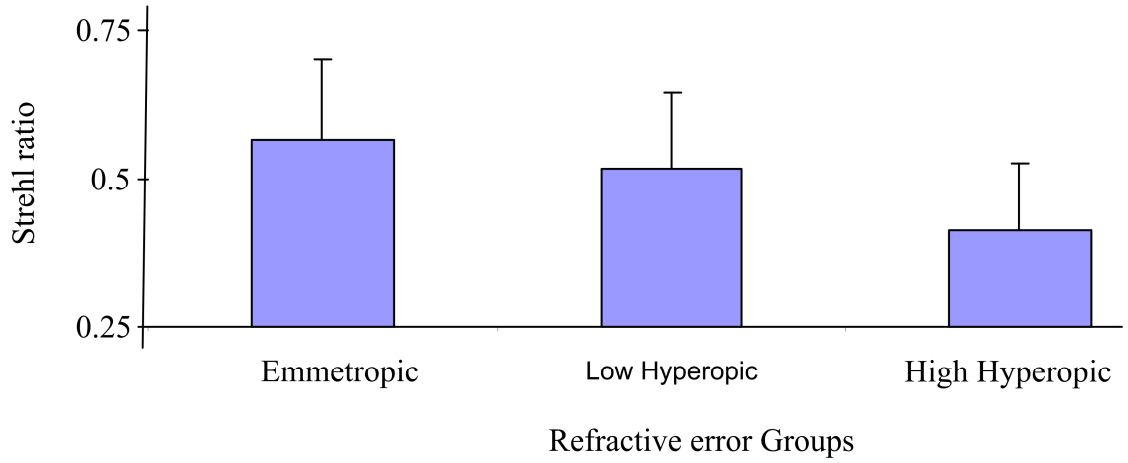

Figure 6:4 Mean values of Strehl ratios for emmetropic, low hyperopic and high hyperopic groups. Strehl ratio of the high hyperopic group was significantly lower than the emmetropic ($p<0.05/3$) and the low hyperopic subjects ($p<0.05/3$) whereas no significant difference in Strehl ratios of the emmetropic and the low hyperopic subjects was observed.

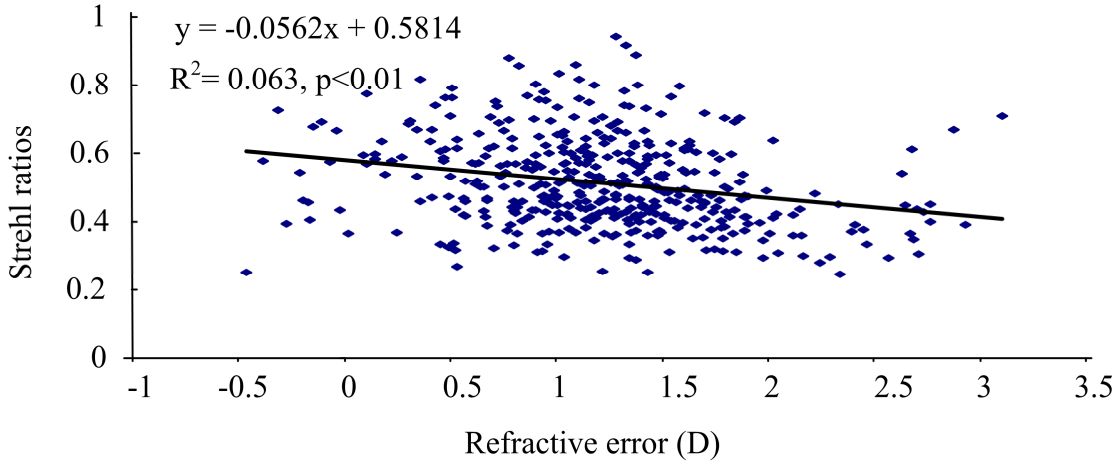

Figure 6:5 Linear fit between Strehl ratios and refractive errors. Significant correlation ($p<0.01$) was found between them. Strehl ratios significantly decreased with the refractive error.

6.4 Discussion

The study of higher order aberrations in a large sample of pre-school children showed the variation of higher order aberrations among individuals with the standard deviation of $0.06\,\mu m$. The mean values of higher order aberrations increased with larger refractive errors and the differences were statistical significant ($p<0.01$) across refractive error groups. The strongest effect was for individuals showing more than +2.00D of hyperopia. The correlation coefficients were small in all of the higher order aberrations; however, the correlations were significant ($p<0.01$). These analyses indicate an association between refractive error and higher order aberrations in the children eyes. These results were also supported by previous results (Chapter 5), where, lower amounts of RMS values for higher order aberrations were associated with better acuity group. If visual acuity is correlated with HOAs, then refractive error is also expected to be correlated with higher order aberrations in pre school sample. These results were not surprising because in Chapter 4 of this thesis, significant correlations were found between higher order aberrations and age. Significant negative correlations were found between age and higher order aberrations. Significant correlations were expected between age and higher order aberrations in our sample because the optical components of the eyes at different ages are systematically different. The optical components of the hyperopic, emmetropic and myopic eyes are also different from each other and that could be the reason for emmetropic subjects having significantly lower amounts of higher order aberrations compared with the hyperopic groups. Brunette et.al[89] studied monochromatic aberration as a function of age from childhood to the advanced age in a population of 114 subjects (mean age 43.2± 24.5 years, range 5 to 82 years) and found higher order aberrations

are at a minimum at the time of emmetropization. This Chapter's results also showed significantly lower amounts of higher order aberrations for emmetropic children. On the other hand, some previous studies in adult's eyes showed no significant correlation between refractive error and higher order aberrations. For example, Cheng et. al[112] studied the relationship between ametropia and higher order aberrations in 200 visually normal eyes and observed no correlation between higher order aberrations and refractive error. Adult eyes are well developed, so the result could be different from the developing eyes of children. In a similar study, Kim et al[79] compared 54 eyes of 36 myopic subjects with greater than -6D of refractive error and 32 eyes of 20 subjects with uncorrected visual acuity of 20/12 and found no significant differences in higher order aberrations. Levy et al[78] also observed no significant difference in higher order aberrations between myopic subjects and supernormal vision (visual acuity 20/15 or better).

Carkeet et. al[77] studied the monochromatic aberrations of 273 Singaporean school children (n= 273± 0.84 years, range 7.9 to 12.7) using a Bausch and Lomb Zywave aberrometer. They also observed slightly but significantly lower value of spherical aberration for low myopes (-3.0D<SE≤-0.5) compared with the high myopes (SE≤-3.0D) (p=0.025) and the emmetropes (-0.5<SE≤+1.0 D) (p=0.001). However, they found almost the same total RMS values for higher order aberrations across refractive error groups (hyperopic, emmetropic, low myopic and high myopic). All other higher order aberrations were not significantly different across the refractive error groups ($p<0.05$). Carkeet et al's study was focused on myopic subjects. The average sample was myopic with a mean spherical equivalent of -1.00D (±1.92STD).

Some previous studies have also reported significant differences in higher order aberrations across refractive error groups. For example, He et al.[90] used *psychophysical* ray-*tracing* technique and measured the monochromatic wavefront aberration of emmetropic and moderately myopic school children and young adults. The ages of the children ranged from 10 to 17 years and the young adults were 18 to 29 years. They further classified the children and adults into emmetropic and myopic groups. They found that the total HOA showed the largest RMS values with myopic children (n=87) followed by myopic adults (n=92), emmetropic children (n=83) and emmetropic adults (n=54). All the inter-group comparisons were significant ($p<0.05$) except the comparison between emmetropic children and myopic adults ($p>0.05$). However, they used natural pupils to calculate ocular aberrations and accommodation was not paralyzed; this approach may have significantly affected the measured aberration levels.

In summary, this study was carried out in a group of visually normal (mainly hyperopic) children across a small age range (3 to 6 years). Although the age range was small, the optics of the eye greatly changes within this period with the mean value of hyperopia decreasing from +1.30D to +1.02 D. We found a significant correlation between higher order aberrations and refractive error and better optical performance in emmetropic subjects than hyperopic subjects. This finding suggests that higher order aberrations decreases at the time of emmetropization.

Chapter 7
Conclusion and Future Work

7.1 Conclusion

In this thesis, an investigation was conducted of Hartmann-Shack images, obtained from a large (n =834) sample of pre-school children in a vision screening program. These subjects were undergoing a specific pattern of emmetropization that were coupled with significant increases in axial length. The ocular growth which continuous after birth involves both anatomical and optical changes such as increased axial length, flattened corneal curvature, and thickened crystalline lens. This study looked at how aberrations varied with age, refractive error and visual acuity. The impact of uncorrelated growth of the optical components of the eye leads to second order aberrations such as refractive error and astigmatism. This study was a further investigation of whether the major anatomical and optical changes in the eye produce different levels of monochromatic aberrations, and whether the ocular aberrations develop differently between eyes of the same individuals. An attempt was also made in further examining how higher order aberrations vary with respect to the magnitude of ametropia. The study led to several conclusions, summarized below.

7.1.1 Symmetry of higher order aberrations between right and left eyes

Seven hundred and ninety six Hartmann-Shack images of 398 subjects (right eyes 398, left eyes 398, mean age 3.93 years ±0.93STD, range 3 to 6 years) were investigated. No significant differences were found between the mean values of higher order aberrations of the right and left eyes. All the higher order aberrations were significantly correlated between the

eyes. When individual Zernike modes from the third to the eighth order were examined, 20 out of 21 Zernike modes with even symmetry were positively correlated and 14 out of 18 Zernike modes with odd symmetry were negatively correlated. However, only 13 out of 21 Zernike modes with even symmetry and 7 out of 18 Zernike modes with odd symmetry were significantly correlated between the right and left eyes. This finding concluded the moderate mirror symmetry in terms of ocular aberrations between eyes of the same individuals.

7.1.2 Development of higher order aberration with age

Hartmann-Shack images of the right eyes of 436 young children were investigated in this study (mean age 3.877± 0.898 years, range 3 to 6 years). No significant difference in the total higher order aberrations (HOA) was observed; however, the p-value was close to the significant level ($p=0.07$). Significant differences in the mean values of the total trefoil and the total eighth order aberrations were found. All the higher order aberrations declined with age and the smallest aberrations were observed for children aged 6 years. Total higher order aberrations, total trefoil, total third order aberration, total seventh order aberration and the total eighth order aberration were significantly correlated ($p<0.05$) with age. This sample shows small variability in the refractive error and contains a large number of individuals of the same age so the result is less affected by the age-related change in refractive error.

7.1.3 Strehl Ratio and Visual acuity

Total of 781 Hartmann-Shack images of 446 children (mean age 3.94± 0.94 years, range 3 to 6 years) were examined in this study (right eye 404 and left eyes 377). The mean RMS values of higher order aberrations increased for lower visual acuity groups; however, the

Bonferonni post-hoc test showed that only the total trefoil was significantly higher for the 6/12 acuity group compared with the 6/6 acuity group. Strehl ratios were found to decline with decreases in visual acuity; however, there were no significant differences in the mean values.

7.1.4 Refractive error and higher order aberration

Four hundred and thirty one right eyes Hartmann-Shack images (mean age 3.89± 0.92 years, range 3 to 6 years) were analyzed to examine the association between refractive error and higher order aberrations. High hyperopes had significantly greater amounts of higher order aberrations compared with the low hyperopes and the emmetropes. Significant negative correlations were found between refractive error and higher order aberrations. Mean Strehl ratios of emmetopes and low hyperopes were significantly greater than that of the high hyperopes. Mean Strehl ratio of emmetropes was greater than that of the low hyperopes; however, there was no significant difference between them.

7.2 Future work

This study can be extended to better understand the development of ocular higher order aberrations in children's eyes. Some interesting studies could be:

7.2.1 Inclusion of subjects from birth to the time of emmetropization

The present study included subjects from 3 to 6 years. It has been found that children are born with hyperopia and the degree of hyperopia decreases with age. Generally refractive error develops from hyperopia through emmetropization to myopia with age. Further studies including subjects in the age range from birth to the time of emmetropization can be useful to

understand the development of ocular aberration with the development of the optical structures of the eye.

7.2.2 Comparison between hyperopes and myopes

This study includes subjects with average refractive errors of +1.19± 0.63D. There were very few myopes and hence could not make a comparison between hyperopes and myopes. Further studies of comparing ocular higher order aberrations between hyperopes, emmetropes and myopes can improve our understanding of the role that aberrations play in the development of refractive error

7.2.3 Repeatability study

There were no repeatability measures on the subjects in this study. A cohort study from birth to the time of emmetropizarion would help to assess the development of ocular aberrations with age.

7.2.4 Comparison of ocular aberration with other devices

In this study, Hartmann-Shack images taken from the Welch Allyn SureSight Autorefractor were calibrated in order to match the lower order aberrations of the retinoscopy. Comparisons of model eyes with known aberration were conducted with the Alcon & Zeiss aberrometer. Further comparative studies of ocular aberrations obtained from Welch Allyn® with other Hartmann-Shack wavefront sensor such as COAS Aberrometer, Bausch and Lomb Zywave aberrometer, WaveScan WavePrint System, or LADARWave® Aberrometer may help to examine the reliability of ocular aberration measurements. The objective SureSight autorefractor measures sphere from +6 to -4.5D and cylinders up to 3D.

Subjects with high hyperopia and high myopia can not be refracted with this instrument. Inclusion of these subjects might better represent the population.

7.2.5 Comparison with model eye

Comparison of real eye aberration with the model eye aberration with known aberration could also be an interesting further study.

References

1. Atchison DA, Smith G. Optics of the Human Eye. *Butterworth-Heinemann*. 2002
2. Edelhauster HF, Ubels JL, Hejny C. The cornea and the sclera. In: Paul L. Kaufman and Albert Alm, eds. Alder's Physiology of the eye 10th ed. *Mosby, Inc.* 2003: 47-114.
3. Beebe DC. The lens. In: Paul L. Kaufman and Albert Alm, eds. Alder's Physiology of the eye 10th ed. *Mosby, Inc.* 2003: 117-118.
4. Charman WN. Wavefront technology: past, present and future. *Contact lens and Anterior Eye*. 2008 (28):75-92
5. Bennett and Rabbetts. Clinical Visual Optics. 3rd ed. *Butterworth-Heinemann:* 1998
6. Sivak JG, Bobier W R. Optical components of the eye: embryology and postnatal development. In: Rosenbloom A, Morgan MW, eds. Pediatric Optometry. Philadelphia, PA: *JB Lippincott Co.* 1992: 31-45.
7. Miller D. Physiologic Optics and Refraction. In: Paul L. Kaufman and Albert Alm, eds. Alder's Physiology of the eye 10th ed. *Mosby, Inc.* 2003: 161-194.
8. Inagaki Y. The rapid change of corneal curvature in the neonatal period and infancy, *Arch Ophthalmol*. 1986; 104:1026
9. Mutti DO et al. Optical and structural development of the crystalline lens in childhood. *Invest Ophthalmol Vis Sci*. 1997; 39:120
10. Goss DA, Van Veen HG, Rainey BB, Feng B. Ocular components measured by keratometry, phakometry, and ultrasonography in emmetropic and myopic optometry students. *Optom Vis Sci.* Jul 1997; 74(7):489-495.
11. Carney LG, Mainstone JC, Henderson BA. Corneal topography and myopia. A cross-sectional study. *Invest Ophthalmol Vis Sci.* Feb 1997; 38(2):311-320.
12. Sorsby A, Leary GA, & Richards MJ. Correlation ametropia and component ametropia. *Vis. Res*. 1962; 2: 309-313.

13. Leat SJ, Shute RH, Westall CA. The developing child and visual system. In: Leat SJ, Shute RH, Westall CA, eds. Assessing children's vision: a handbook. Wooburn,Ma. *Butterworth-Heinemann*. 1999: 1-36.

14. Banks M. Infant refraction and accommodation. *Int. Ophthal. Clin.* 1980; 20(1): 205-232

15. Hirsch MJ. The refraction of children. In Hirsch MJ and Wicks JE, Vision of children. *Philadelphia, Chilton.* 1963

16. Gwiazda J, Thorn F, Bauer J, and Held R. Emmetropization and the progression of manifest refraction in children followed from infancy to puberty. *Clinical Vision Science*. 1993; 8: 337-344.

17. Atkinson J, Braddick O, and French J. Infant astigmatism: Its disappearance with age. *Vis. Res.* 1980; 20: 891-893.

18. Grosvenor T. Primary care optometry. 4th ed. *Butterworth-Heinemann:*2007

19. Glasser A, Kaufman PL, Accommodation and presbyopia. In: Paul L. Kaufman and Albert Alm, eds. Alder's Physiology of the eye 10th ed. *Mosby, Inc.* 2003: 197-233.

20. Saunders H. A longitudinal study of the age dependence of human ocular refraction. 1. Age-dependent changes in the equivalent sphere. *Ophthal. Physiol.Opt.,* 1986; 6: 39-46

21. Saunders H. Age-dependence of human refractive errors. *Ophthal. Physiol. Opt*.,1,: 159-74

22. Lee KE, Klein BEK, and Klein R. Changes in refraction over ten-year in an adult population. The Beaver Dam Eye Study. *Invest Ophthalmol Vis Sci* .August 2002; 43, No.8:2566-2571

23. Wong TY, Foster PJ, Hee J, et al. Prevalence and risk factors for refractive errors in adult Chinese in Singapore. *Invest Ophthalmol Vis Sci.* Aug 2000; 41(9):2486-2494.

24. Attebo K, Ivers RQ, Mitchell P. Refractive errors in an older population. the Blue Mountains Eye Study. *Ophthalmology.* Jun 1999; 106(6):1066-1072.

25. Hyman L. Myopic and hyperopic refractive error in adults: an overview. *Ophthalmic Epidemiol.* Jul-Aug 2007; 14(4):192-197.

26. Suryakumar R, Bobier WR. The manifestation of noncycloplegic refractive state in pre-school children is dependent on autorefractor design. *Optom Vis Sci* 2003; 80: 578-586.

27. Howland HC, and Sayles N. Photorefractive measurements of astigmatism in infants and young children. *Invest Ophthalmol Vis Sci*. 1984; 25(1), 93-102.

28. Atkinson J, Braddick O, and French J. Infant astigmatism: Its disappearance with age. *Vis. Res.* 1980; 20: 891-893.

29. Held R, Mohindra I, Gwiazda J, and Brill S. Astigmatism in infants. *Science:* October 1978; 202: 329-331.

30. Cowen L, Bobier WR. The Pattern of Astigmatism in a Canadian Preschool Population. *Invest Ophthalmol Vis Sci.* 2003; 44:4593–4600

31. Gwiazda J, Scheiman M, Mohindra I, Held R. Astigmatism in children: changes in axis and amount from birth to six years. *Invest Ophthalmol Vis Sci* 1984; 25:99

32. Dobson V, Fulton AB, and Sebris S. Cycloplegic refractions of infants and young children: The axis of astigmatism. *Invest Ophthalmol Vis Sci*. 1984; 25, 83-87.

33. Booth RG, Dobson V, Teller DY. Post natal development of vision in human and nonhuman primates. *Ann Rev Neurosci* 1985; 8:495

34. Teller DY. First glances. The vision of infants. *Invest Ophthalmol Vis Sci* 1997; (38), No. 11

35. Banks MS, Bennett PG: Optical and photoreceptor immaturities limit the spatial and chromatic vision of human neonates. *J Opt Soc Am 5A:* 1988, 2059

36. Atkinson J. Human visual development over the first 6 months of life. A review and a hypothesis. *Human Neurobiology*. 1984; 3:61-74.

37. Maeda N. Wavefront technology in ophthalmology. Current opinion in ophthalmology. *Lippincott Williams and Wilkins.* August 2001; 12(4): 294-299

38. Geary JM. Introduction to wavefront sensors. *SPIE-The International Society of Optical Engineering.* Vol. TT 18

39. Maeda PY. Zernike Polynomials and Their Use in Describing the Wavefront Aberrations of the Human Eye. Stanford University: Psych 221/EE 362 Applied Vision and Imaging Systems Course Project, Winter 2003

40. Smirnov MS. Measurement of the wave aberration of the human eye. *Biophys.* 1961; 6:52-66.

41. Howland HC, Howland B. A subjective method for the measurement of the monochromatic aberrations of the eye. *J Opt Soc Am*. 1977; 67:1508–1518.

42. Walsh G, Charman WN, Howland HC. Objective technique for the determination of monochromatic aberrations of the human eye. *J Opt Soc Am A*. 1984; 1:987-992.

43. Mierdel P, Krinke HE, Wiegand W, Kaemmerer M, Seiler T. A measuring device for the assessment of monochromatic aberrations in human eyes. *Ophthalmologe* 1997; 94: 441-445.

44. Liang J, Grimm B, Goelz S, Bille JF. Objective measurement of wave aberrations of the human eye with the use of a Hartmann–Shack wave-front sensor. *J Opt Soc Am A* 1994; 11:1949–57.

45. Burns SA. The spatially resolved refractometer. *J Refract Surg* 2000, 16:S566-9

46. Yoon G. Wavefront Sensing and Diagnostic Uses. Adaptive Optics for Vision Science. Principles, Practices, Design, and Applications. Edited by Jason Porter, Hope M. Queener, Julianna E. Lin, Karen Thorn, and Abdul Awwal. *A John Wiley and Sons, Inc*. 2006

47. Wyant JC, Creath K. Basic Wavefront Aberration Theory for Optical Metrology. Applied Optics and Optical Engineering. Vol. XI. *Academic Press, Inc*.1992

48. Pedrotti FL, Pedrotti LM, Pedrotti LS. Introduction to Optics. 3rd ed. *Prentice-Hall,* 1993

49. Larsen JS. The sagittal growth of the eye. IV. Ultrasonic measurement of the axial length of the eye from birth to puberty. *Acta Ophthalmologica*. 1971; 49: 873-886.

50. Robinson BE, Bobier W R, Martin E. Oxford County preschool vision screening: prevalence of vision problems. *Can J Optom* 1999; 62: 19-25.

51. Robinson BE, Bobier W R, Martin E, Bryant L. Measurement of the validity of a preschool vision screening program. *Am J Public Health* 1999; 89: 193-198.

52. Shankar S, Bobier WR. Corneal and Lenticular Components of Total Astigmatism in a Preschool Example. *Optom.Vis.Sc*i. 2004; 81: 536-542.

53. Suryakumar R, Bobier WR. Gain and movement time of convergence-accommodation in preschool children. *Optom.Vis.Sc*i.2004, 81: 835-843.

54. Shankar S, Evans MA, Bobier WR. Hyperopia and emergent literacy of young children: pilot study. *Optom.Vis.Sc*i. 2008; 84: 1031-1038.

55. Welch Allyn SureSight Autorefractor Manual. Skaneateles Falls, NY.

56. Welch Allyn SureSight Autorefractor Service Manual. Skaneateles Falls, NY.

57. Vricella M, FitzGerald DE, and Krumholtz I. Effectiveness of the Welch Allyn SureSight Autorefractor as a Screening Tool in a Sample of Children Aged 3-69 Months. *Journal of Behavioral Optometry*. 2002; 13; No. 5; pp. 124

58. Cardonnier M, Maertelaer V. De. Comparison between two hand-held autorefractors: the Sure-Sight and the Retinomax. Strabismus. 2004; 12; No. 4; pp. 261–274

59. Aldaham SM. visual acuity testing and refractive error analysis in pre-school children. Master's thesis University of Waterloo. 2005.

60. Visual Development Unit UoC. The Cambridge crowding cards. London,UK: *Clement Clarke International Ltd.* 1987. Catalog Number 4116025.

61. Thibos LN, Applegate RA, Schwiegerling JT, et al. Standards for reporting the optical aberrations of eyes. In: MacRae SM, Krueger RR, Applegate RA, editors. Customized corneal ablation; the quest for supervision. Thorofare, NJ: Slack, 2001:348 –361.
62. Fleck A, Bobier WR. The development of a hand-held wavefront sensor. Presented at the Annual Graduate conference, University of Waterloo, April 2004.
63. Marcos S, Burns S.A. On the symmetry between eyes of wavefront aberration and cone directionality. *Vis. Res*.2000;40:2437–2447
64. Burns SA, He JC, and Marcos S: The influence of cone directionality on optical image quality. *Invest Ophthalmol Vis Sci* (*Supplement*).1998; 39: 203.
65. Miller DT, Williams DR, Morris GM, and Liang J: Images of the cone photoreceptors in the living human eye. *Vis. Res.* 1996; 36:1067–1079.
66. Guirao A, Gonzalez C, Redondo M, Geraghty E. Norrby S, and Artal P. Average optical performance of the human eye as a function of age in a normal population. *Invest Ophthalmol Vis Sci*. January 1999; 40, No. 1
67. de Vries J. Anisometropia in children: Analysis of a hospital population. *Br J Ophthalmol* 1985; 69: 504-507
68. Hirsch MJ. Anisometropia: A preliminary report of the Ojai Longitudinal study. *Am J Optom Arch Am Acad Optom*.44(9): 581-585
69. Larsson EK, Holmstrom GE. Development of astigmatism and anisometropia in preterm children during the first 10 years of life. *Arch Ophthalmol*. November 2006;124
70. Ingram RM, Barr A. Changes in refraction between the ages of 1 and 3 1/2 years. *Br J Ophthalmol*. 1979; 63:339-342.
71. Abrahamsson M, Fabian G, Andersson AK, and Sjostrand J. A longitudinal study of a population based sample of astigmatic children. II. The changeability of anisometropia. *Acta Ophthalmologica*. 1990; 68, 435-440.
72. Wang L, Koch DD. Ocular higher-order aberrations in individuals screened for refractive surgery. *J Cataract Refract Surg.* October 2003; 29

73. Wang L, Dai E, MD, Koch DD, MD and Nathoo A. Optical aberrations of the human anterior cornea. *J Cataract Refract Surg.* August 2003; 29
74. Porter J, Guirao A, Cox IG, Williams DR. Calculated impact of higher-order monochromatic aberrations on retinal image quality in a population of human eyes. *J. Opt. Soc. Am. A.* January 2002; 19, No. 1
75. Lombardo M, Lombardo G, Serrao S. Intraocular high-order corneal wavefront aberration symmetry. *J. Opt. Soc. Am. A*, April 2006; 23; No.4
76. Zadok D, Levy Y, Segal O, Barkana Y, Morad Y, Avni I. Ocular higher-order aberrations in myopia and skiascopic wavefront repeatability. *J Cataract Refract Surg*.June 2005; 31
77. Carkeet A, Luo HD, Tong L, Saw SM, Tan DTH. Refractive error and monochromatic aberrations in Singaporean children. *Vis. Res*. 2002 (42): 1809–1824
78. Levy Y, Segal O, Avni I, Zodak D. Ocular Higher-order Aberrations in Eyes with Supernormal Vision. *Am J Ophthalmol.* February 2005; 139, No.2
79. Kim M, Lee YG, Seo KR, Kim Ek, Lee HK. Comparison of higher-order aberrations between eyes with natural supervision and highly myopic eyes in Koreans. *Kor J Ophthalmol*. 2007; 21, No. 2
80. Qin XJ, Margrain TH, To CH, Brombam N, Guggenbeim JA. Anisometropia is independently associated with both spherical and cylindrical ametropia. *Invest Ophthalmol Vis Sci.* November 2005; 46, No. 11
81. Artal P, Ferro M, Miranda I, Navarro R. Effects of aging in retinal image quality. *J. Opt. Soc. Am. A.* July 1993;10(7):1656-1662
82. McLellan JS, Marcos S, and Burns SA. Age-related changes in monochromatic wave aberrations of the human eye. *Invest Ophthalmol Vis Sci.* May 2001;42(6):1390-1395
83. Salmon TO, Van de Pol C. Normal-eye Zernike coefficients and root-mean-square wavefront errors. *J cataract surg*. December 2006; 32: 2065-2074.
84. Fujikado T, Kuroda T, Ninomiya S. Maeda N, Tano Y, Oshika T, Hirohora Y. Mihashi T. Age-related Changes in Ocular and Corneal Aberrations. *Am. J Ophthalmol*. 2004;138, No. 1

85. Kuroda T, Fujikado T, Ninomiya S, Maeda N, Hirohora Y, and Mihashi T. Effect of aging on ocular light scatter and higher order aberrations. *J Refract Surg.* Sep-Oct 2002; 18(5):S598-602.
86. Atchison DA, Markwell EL. Aberrations of emmetropic subjects at different ages. *Vis. Res*. 2008; 48: 2224–2231
87. Jesson M, Arulmozhivarman P, Ganasen AR. Higher order aberrations of the eye in a young Indian population. *Asian J. of ophthalmol.* 2004; 6(2):10-16
88. Calver RI, Cox MJ, Elliott DB. Effect of aging on the monochromatic aberrations of the human eye. *J. Opt. Soc. Am. A,* September 1999; 16, No. 9
89. Brunette I, Bueno JM, Parent M. Hamam H, Simonet P. Monochromatic Aberrations as a Function of Age, from Childhood to Advanced Age. *Invest Ophthalmol Vis Sci.* December 2003; 44, No. 12
90. He JC, Sun P, Held R, Thorn F, Sun X, and Gwiazda JE. Wavefront aberrations in eyes of emmetropic and moderately myopic school children and young adults. *Vis. Res.* 2002; 42, 1063–1070
91. Applegate RA, Howland HC, Sharp RP, Cottingham AJ, Yee RW. Corneal aberrations and visual performance after radial keratomy. *J. Refract Surg* 1998, 14: 397-407
92. Ninomiya S, Maeda N, Kuroda T, Fujikado T, Tano Y. Comparison of ocular higher-order aberrations and visual performance between photorefractive keratectomy and laser in situ keratomileusis for myopia. *Seminars in Ophthalmology*. 2003; 18, No. 1: 29–34
93. Oshika T, Klyce SD, Applegate RA, Howland HC, Danasoury MAE. Comparison of corneal wavefront aberrations after photorefractive keratectomy and laser in situ keratomileusis. *Am. J Ophthalmol* 1999, 127: 1-7
94. Yamabe N, Miyata K, Samejima T. Hiraoka T, Kiuchi T, Okamoto F, Hirohara Y, Mihashi T, Oshika T. Ocular Higher-Order Aberrations and Contrast Sensitivity after Conventional Laser in Situ Keratomileusis. *Invest Ophthalmol Vis Sci.* November 2004;45, No. 11

95. Naoyuki M. Wavefront technology in ophthalmology. *Current opinion in ophthalmology*. Aug 2001; 12(4):294-299
96. Seiler T, Mrochen W, Kaemmerer M. Operative correction of ocular aberrations to improve visual acuity. *J Refract Surg* 2000, 16: S619-622.
97. Mrochen M, Kaemmerer M, Seiler T. Wavefront-guided laser in situ Keratomilesusis. *J. refract. Surg* 2000, 16: 116-121.
98. Liang J, Williams DR, Riller DT. Supernormal vision and high-resolution imaging through adaptive optics. *J. Opt. Soc. Am. A*. November 1997; 14 No.11
99. Agarwal A. Aberropia defined. *Cataract and refractive surgery today Europe*. February 2009.
100. Applegate RA, Hilmantel G, Howland HC, Tu EY, Starck T, Zayac EJ. Corneal first surface optical aberrations and visual performance. *J Refract Surg* 2000; 16:507–514
101. Hong X, Thibos LN, Bradley A, et al. Impact of monochromatic aberrations on polychromatic image quality and vision. *Invest Ophthalmol Vis Sci.* 2001; 42:S162
102. Williams CS, Becklund OA. Introduction to the Optical Transfer Function. New York: *John Wiley*; 1989.
103. Anonymous. Why a journal devoted to screening. Screening, 1, 1992: 1-3.
104. Atkinson J. Infant vision screening: Prediction and prevention of strabismus and amblyopia from refractive screening in the Cambridge photorefraction programme. In Simons,K.(Eds), Early visual development normal and abnormal, 1st ed.Oxford: *Oxford University Press.* 1993:335-348
105. Wang Y, Zhao K, Jin Y, Niu Y, Zuo T. Changes of higher order aberration with various pupil sizes in the myopic eye. *J Refract Surg 2003*; 19(suppl 2):S270 –S274.
106. Thibos LN, Hong X, Bradley A, Applegate RA. Accuracy and precision of objective refraction from wavefront aberrations. *Journal of Vision.* 2004; 4, 329-351
107. Faylinejad A. Computational model for predicting the visual acuity from the wavefront aberration measurement, a thesis University of Waterloo, June 2009.
108. Paquin MP, Hamam H, Simonet P. Objective measurement of optical aberrations in myopic eyes, *Optom.Vis.Sc*i. May 2002; 79, No. 5

109. Bueno JM, Priest D, and Campbell MCM. Optical aberrations of the eye as a function of refractive error in young subjects. *OSA,* Annual Meeting, Optics and Photonics News (supp). 2000; 11, pg. 100

110. Martinez AA, Sankaridurg PR, Naduvilath TJ and Mitchell P. Monochromatic aberrations in hyperopic and emmetropic children. *Journal of Vision*. 2009; 9(1):23, 1–14

111. Wei RH, Lim L, Chan WK, Tan DTH. Higher order ocular aberrations in eyes with myopia in a Chinese population. *J Refract Surg.* September 2006; 22

112. Cheng X, Bradley A, Hong X, Thibos LN. Relationship between refractive error and monochromatic aberrations of the eye *Optom.Vis.Sc*i. January 2003; 80, No.1

113. Kirwan C, O'Keefe M, Soeldner H. Higher Order Aberrations in Children. *J. opt. Soc. Am. A.* January 2006; 141, Issue 1: 67-70

114. Llorente L, Barbero S, Cano D, Dorronsoro C, and Marcos S. Myopic versus hyperopic eyes: axial length, corneal shape and optical aberrations. *Journal of Vision*. 2004; 4, 288-298